This is to certify that the
thesis entitled

THE EFFECT OF INSULIN-LIKE GROWTH FACTOR 1 ON
CHANGES IN PROLIFERATION-RELATED GENE EXPRESSION
IN BOVINE MAMMARY EPITHELIAL CELLS

presented by

MICHAEL ALAN JACOBSEN

has been accepted towards fulfillment
of the requirements for the

M.S. degree in Animal Science

Major Professor's Signature

8-17-07

Date

THE EFFECT OF INSULIN-LIKE GROWTH FACTOR 1 ON CHANGES IN PROLIFERATION-RELATED GENE EXPRESSION IN BOVINE MAMMARY EPITHELIAL CELLS

By

MICHAEL ALAN JACOBSEN

A THESIS

Submitted to
Michigan State University
In partial fulfillment of the requirements
For the degree of

MASTER OF SCIENCE

DEPARTMENT OF ANIMAL SCIENCE

2007

THE EFFECT OF INSULIN-LIKE GROWTH FACTOR 1 ON CHANGES IN PROLIFERATION-RELATED GENE EXPRESSION IN BOVINE MAMMARY EPITHELIAL CELLS

By

MICHAEL ALAN JACOBSEN

ABSTRACT

Insulin-like growth factor 1 (IGF-1) is a potent mitogen for mammary epithelial cells. My objective was to determine if IGF-1 treatment alters the expression of genes in the MAC-T bovine mammary epithelial cell line in a manner consistent with increased proliferation. Cells were treated with 0 or 100 ng/mL of IGF-1 for 8 or 24 hours. Gene transcript abundance was measured with a bovine metabolism microarray of 2360 genes. IGF-1 increased cell confluency by 40% after 24 hr of treatment ($P < 0.05$). IGF-1 altered the expression ($P < 0.05$) of 89 genes after 8 hours (70 increased, 18 decreased) and 184 genes after 24 hours (139 increased, 45 decreased). IGF-1 altered the expression of several regulatory genes that might increase cell proliferation and several metabolic genes to support increased proliferation. The fold-changes of 9 of 10 genes as measured with RT-PCR were similar to those with microarray analysis, although the statistical significance of the change was the same for only 6 of the genes. In conclusion, IGF-1 alters the expression of proliferative and metabolic genes in a manner consistent with increased cell proliferation.

For my beautiful wife Ruth

ACKNOWLEDGEMENTS

First, I would like to thank my advisor, Dr. Michael VandeHaar, without whos guidance, support, and grace this degree would never have been possible. I would also like to extend my gratitude to my committee, Dr. Smith, Dr. Weber-Neilsen, and Dr. Sordillo, for their input and support. Second, I would like to thank Jim Liesman for his invaluable statistical and technical support. Next, I give my appreciation to Chris Colvin, Sue Sipkofsky, Xiaoning Rei, Patty Weber and Janet Ireland for the use of their lab equipment. I would also like to thank my fellow and former lab mates, Myunggi Baik, Jinjong Bong, Laurie Davis-Rinker, Brett Etchebarne, and Jianguo Li for their encouragement. Finally, I would like to give my deepest gratitude to my family, John, Susan, and Katie, and my wife Ruth who have kept me focused on completing my M.S. degree.

TABLE OF CONTENTS

LIST OF TABLES

LIST OF FIGURES

LIST OF ABBREVIATIONS

ADG	Average daily gain
BSA	Bovine serum albumin
cDNA	Complementary deoxyribonucleic acid
DEPC	Diethylpropyl carbonate
DMSO	Dimethyl sulfoxide
DNA	Deoxyribonucleic acid
dNTP	Deoxyribonucleotide triphosphates
DTT	Dithiothreitol
E	Estrogen
ECM	Extracellular matrix
EtOH	Ethanol
FBS	Fetal bovine serum
GH	Growth hormone
hr	hours
IGF-1	Insulin-like growth factor 1
IGF-2	Insulin-like growth factor 2
IGFBP	Insulin-like growth factor binding protein
IRS	Insulin related substrate
min	minutes
TEB	Terminal end buds

JAK	Janus kinase
MAPK	Mitogen-activated protein kinase
MDGI	Mammary-derived growth inhibitor
mRNA	Messenger ribonucleic acid
PBS	Phosphate buffered saline
PI3K	Phosphotidylinositol -3 kinase
qRT-PCR	Quantitative reverse-transcriptase polymerase chain reaction
STAT	Signal transducer and activator of transcription

INTRODUCTION

Prepubertal mammary development in the dairy heifer sets the foundation for future epithelial cell growth and activity. Sinha and Tucker (1969) found that between 3 months and 9 months of age, the mammary parenchyma grows at a 3-fold greater rate than body growth. Because dairy heifer rearing costs account for 20% of farm costs, dairy scientists have studied the effect of feeding heifers for an average daily gain (ADG) of greater than 1.0 kg/d to decrease rearing times. In an experiment studying the effect of ADG greater than 1 kg/d on body growth and mammary development in dairy heifers between the ages of 11 and 23 weeks, Davis-Rinker (2005) found that heifers fed for an ADG of 1.1 kg/d possessed more total mammary gland mass but less parenchyma per unit of body mass than heifers fed for 0.7 kg/d. Davis-Rinker then stained the mammary parenchymas of heifers from both treatments for Ki-67, a proliferation-related cell marker, and counted the number of stained cells. The mammary parenchymas of heifers fed for an ADG of 1.1 kg/d had 30% less Ki-67-labeled cells than the parenchymas of heifers fed for 0.7 kg/d, demonstrating a decrease in cell proliferation. The high-gain diet increased circulating concentrations of insulin-like growth factor 1 (IGF-1) by 77%. IGF-1 is considered to be a major regulator of proliferation. For example, after infusing the udders of prepubertal heifers with 10 μg IGF-1 for 7 days, Silva (2002) discovered that IGF-1-infused quarters contained 52% more proliferating epithelial cells than saline-infused quarters. Therefore, a paradox exists in which heifers fed for high rates of gain have higher circulating levels of IGF-1 but decreased mammary parenchyma development compared to heifers fed for more moderate rates of gain. The current state of knowledge on mammary development, effects of diet, and IGF-1 are discussed in the literature review.

IGF-1 can affect proliferation via a number of different possible mechanisms. IGF-1 binding to mammary epithelial cells could be altered by changes in the presence and concentration of IGF binding proteins (IGFBP) in the mammary parenchyma. Weber et al. (2000) found that IGFBP2 expression was increased and IGFBP1 expression was decreased in the parenchymas of heifers fed for high rates of gain. IGF-1 can also influence or be influenced by other hormones. Leptin impairs the proliferative effect of IGF-1 in mammary epithelial cells as compared with cells treated with only IGF-1 (Silva, 2002). However, there are other possible mechanisms, such as gene expression changes, protein synthesis and modification changes, IGF-1 receptor number changes, and phosphorylation changes. To further explore the proliferative effect of IGF-1 on bovine mammary epithelial cells, I examined the changes in gene expression due to IGF-1 stimulation. To our knowledge, no one had previously explored the effect of IGF-1 on gene expression in bovine mammary epithelial cells. Furthermore, our lab has the means (the BMET microarray; Etchebarne, 2005) to study gene expression changes. The BMET microarray contains all of the known genes associated with metabolism and proliferation in the cow. Four spots per gene on the BMET array provides the technical replication for reducing possible effects of probe spot and spot position on the final results. By finding which genes are directly altered by IGF-1, we now have a foundation to explore which genes are altered by IGF-1 in conjunction with other factors (feeding levels, hormones, puberty, etc.).

To localize changes in gene expression to mammary epithelial cells, we used the MAC-T cell line. The MAC-T cell line is an immortalized bovine mammary epithelial cell line that was developed by transfecting the SV40 T-antigen into epithelial cells taken from a lactating Holstein cow (Huynh et al., 1991). To test my hypothesis, it is critical that the cells proliferate in response to IGF-1. Primary cells can undergo senescence, in which they stop proliferating after being passaged too many times (Matitashvili et al, 1997). The MAC-T cell line is a pure population of bovine mammary epithelial cells, albeit with modifications, and, most importantly, MAC-T cells consistently increase proliferation in response to IGF-1. In fact, in my preliminary results, MAC-T cells treated with 100 ng/mL IGF-1 synthesized DNA at greater than 3 times the rate of control cells. Therefore, much of the signaling pathways are likely still intact in the MAC-T cells.

Therefore, my hypothesis is that IGF-1 alters the expression of genes in a manner consistent with increased proliferation in bovine mammary epithelial cells. To test this hypothesis, my objective was to determine if IGF-1 treatment for 8 and 24 hours alters the transcript abundance of genes in the MAC-T bovine mammary epithelial cell line in a manner consistent with increased proliferation. I used the BMET microarray, an oligonucleotide array constructed entirely of genes related to proliferation and metabolism in the cow.

Literature Review

Overview of mammary development

Mammary development has been described in detail by Williams and Daniel (1983) and Akers (2000). As these authors explain, mammary gland development in the bovine fetus is initiated at 30 days of gestation. Ectodermal cells combine together to form the mammary streak. As the fetus ages, the rudimentary gland progresses through the crest, hillock, bud, and sprout stages. The primary sprout appears as a solid mass of cells but it canalizes into a hollow structure containing an epithelial cell border two to three layers thick that will become the future milk cistern. Secondary sprouts, which will become the large ducts emptying into the milk cistern, extend from the primary sprout at around day 90 in the fetus. The mammary fat pad appears at the same time as the primary and secondary sprouts and the teat begins to form soon after the development of the sprouts. At birth, the streak canal, milk cistern and a few ducts budding from the milk cistern are present. As the heifer ages, the ducts extend into the fat pad, and each duct gives rise to subtending ducts.

The parenchyma develops at the same rate as the body until 3 months of age. From 3 months to about the third or fourth estrous cycle, the parenchyma grows at roughly three times the rate of the body (Sinha and Tucker, 1969). In rodents, most of the growth is ductal in nature, with few alveolar-like structures branching off the ducts. Ductal extension occurs via the rapid invasion of the terminal end buds (TEB) into the mammary fat pad with very few branches until the edge of the fat pad is reached (Williams and Daniel, 1983). However, prepubertal mammary development in heifers involves less extensive growth into the mammary fat pad from the nipple and a higher degree of branching from the ducts into a loose sheath of connective tissue, giving rise to a broccoli-like appearance, as shown by Ellis and Capuco (2002) using computerized tomography. Extensive branching was apparent in regions of actively proliferating epithelial cells and occurred in conjunction with ductal elongation. Furthermore, branching occurred along the ducts within these regions of 'terminal ductal units' as they were labeled by the researchers. After puberty, the parenchymal growth rate again matches that of the body until pregnancy (Sinha and Tucker, 1969). The vast majority of mammary parenchyma growth occurs during pregnancy.

The amount of DNA in a tissue is considered to be proportional to the number of cells in the tissue. Thus, an increase in the DNA content indicates an increase in cell numbers in the mammary parenchyma, and one way to study cell proliferation is to measure the DNA content of a tissue. Another method to determine cell proliferation is to measure radioisotope-labeled thymidine incorporation, which is considered to be a "snapshot" view of cell proliferation. Proliferating cells take up nucleotides for DNA replication during the S-phase of the cell cycle; therefore, this assay provides an estimate of cells undergoing DNA replication during a particular period of time. Weber et al. (2000) measured tritiated thymidine incorporation in primary bovine mammary epithelial cells that were treated with mammary extracts prepared from prepubertal heifers fed for a high or a low rate of gain. They discovered that thymidine incorporation was increased by about 40% in cells treated with extracts from the low rate-of-gain heifers compared to cells treated with extracts from heifers fed for high rates of gain. Therefore, measuring DNA content provides a basis for measuring mammary development.

Effect of diet on mammary development in prepubertal dairy heifers

Feeding for higher rates of gain decreases rates of prepubertal mammary development relative to body growth (for review, see Sejrsen and Purup, 1997; Sejrsen et al., 2000; and Akers, 2002). Prepubertal heifers reared at an average daily gain (ADG) above 1.0 kg/d have less parenchymal mass at puberty than heifers reared at 0.7 kg/d (Sejrsen et al., 1982). In another study, Harrison et al. (1983) showed that heifers reared at 1.1 kg/d contained 68% less secretory tissue than in heifers reared at 0.7 kg/d. Other studies have confirmed this effect (Little and Kay, 1979, Petitclerc et al., 1984 and Stelwagen and Grieve, 1990), although it has not been universally proven (Van Amburgh et al., 1998). Meyers et al. (2006) measured mammary gland weight and DNA content of mammary gland samples from heifers fed a diet for either restricted gain (0.65 kg/d) or high gain (0.95 kg/d). Heifers were slaughtered at 50-kg increments from 100 kg to 350 kg of body weight. Parenchymal weight and DNA content was decreased in heifers fed the high-gain diet versus heifers fed the restricted diet. When age at tissue collection was added as a covariate to the model, the diet effects disappeared. They argued that the observations of adverse effect of diet on mammary development were actually due to age of the heifer at tissue harvest. Davis-Rinker (2005) discovered that heifers fed for 1.1 kg/d between 11 weeks and 23 weeks of age had 23% less grams parenchyma per unit body weight, and a 30% reduction of Ki-67-labeled epithelial cells (indicating decreased cell proliferation). Therefore, the full effects of high rates of gain on mammary development are still being explored.

Sejrsen et al. (1983) examined the effects of feeding for high or moderate rates of gain on serum growth hormone (GH) as a basis for understanding mammary growth.

Heifers fed for restricted rates of gain (0.7 kg/d) had higher concentrations of GH in serum than those fed for rapid growth. Serum GH concentrations were positively correlated with parenchyma mass and negatively correlated with extraparenchymal adipose mass. Feeding for rapid growth led to a reduction in hepatic GH mRNA abundance (Smith et al., 2002). VandeHaar et al. (1995) measured the effect of negative energy balance on hepatic and luteal IGF-1 expression in post pubertal heifers. Heifers in negative energy balance had increased serum GH concentrations and decreased serum IGF-1 levels. They also found that hepatic IGF-1 mRNA levels were also decreased in heifers in negative energy balance. Radcliff et al., (2004) discovered that prepubertal heifers fed for high rates of gain had increased levels of serum IGF-1. However, this difference disappeared after the heifers had attained puberty. High rates of gain also increased liver IGF-1 mRNA abundance, and rate of gain was positively correlated with serum IGF-1 concentrations ($r = 0.60$, $P < 0.01$). Davis-Rinker (2005) discovered that heifers fed for an ADG of 1.1 kg/d had a 73% greater circulating IGF-1 concentration than heifers fed for 0.7 kg/d during the same time period. Therefore, as shown in figure 1, high-energy diets promote high rates of body growth and increase serum IGF-1 concentrations in prepubertal heifers; however, high rates of gain lead to diminished mammary parenchymal development. The reasons for this paradox are not clear. Perhaps other hormones, such as leptin, are involved (Silva et al., 2005). I hope to find gene pathways that serve as targets to understand this paradox.

Figure 1. High-energy diets fed to prepubertal heifers increase body growth and IGF-1 production in prepubertal dairy heifers. IGF-1 also stimulates mammary development. However, feeding high-energy diets to prepubertal heifers diminishes mammary parenchymal development.

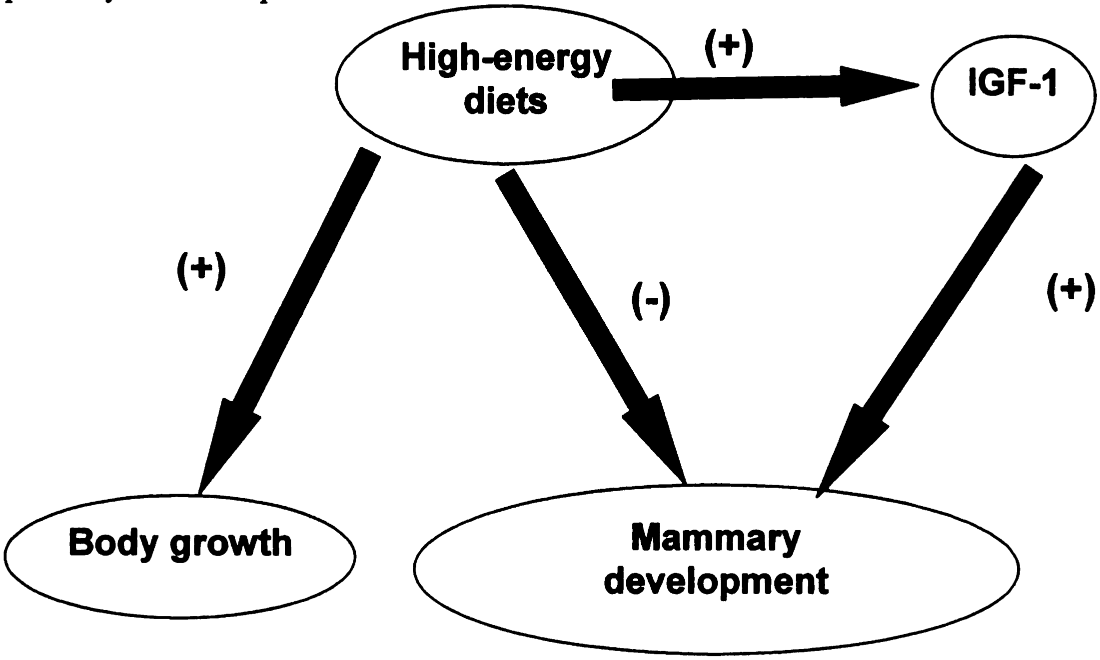

The Somatomedin Hypothesis

Growth hormone (GH) increases body tissues growth; yet the theory explaining the mechanism of GH action changed numerous times over the past sixty years. The initial theory that GH stimulates growth through an intermediary factor was proposed in the 1950's when it was demonstrated that GH treatment on costal cartilage slices only minimally affected cartilage growth (Daughaday and Reeder, 1966). Given that hypophysectomy reduces bone growth and GH administration re-establishes growth in hypophysectomized animals (Denko and Bergenstal, 1955), it was suggested that GH affects growth via another signal, termed "sulfation factor". This "sulfation factor" was partial purified from the serum of acromegalic patients and could mimic the mitogenic effects of GH. Thus, it was renamed "somatomedin" because it mediated the action of

GH on growing tissues (Daughaday et al., 1972). Six years later, IGF-1 and IGF-2 were purified and found to be the "sulfation factor" that affected growth in rats. Furthermore, IGF-1 levels were found to be affected by GH administration, thereby cementing its identity as the proposed "sulfation factor" (Klapper et al., 1983). Thus, the original hypothesis stated that GH was released from the pituitary gland and traveled to the liver, where it stimulated the release of IGF-1. IGF-1 in turn provided negative feedback on GH production in the pituitary gland.

However, this theory was questioned when it was found that IGF-1 was produced by several fetal tissues (D'Ercole et al., 1980). Furthermore, IGF-1 was found to be expressed in numerous tissues other than the liver. This prompted the idea that IGF-1 could be an autocrine/paracrine factor and that GH could stimulate localized production of IGF-1. Even this view may not fully explain IGF-1 production since GH-dependent IGF-1 synthesis in the mammary gland has never been explicitly demonstrated (Glimm et al., 1992). Therefore, according to the most recent proposal of the somatomedin theory, GH travels from the pituitary gland to the liver where it induces IGF-1 synthesis and release. Furthermore, GH can bind to GH receptors on other tissues and perform various functions. The liver synthesized IGF-1 is then bound to IGFBPs and travels to the target tissues, where it initiates primarily proliferative and survival signaling pathways. Finally, IGF-1 is produced by local tissues and acts upon the target tissue, as shown in Figure 2 on page 10. For many tissues, serum IGF-1 is probably less important than local IGF-1 (Le Roith, 2001). However, because the bovine mammary gland lacks GH receptors (Glimm et al., 1992), serum IGF-1 may exert a greater effect on proliferation.

Figure 2. The current form of the somatomedin hypothesis. Taken from Akers, 2006.

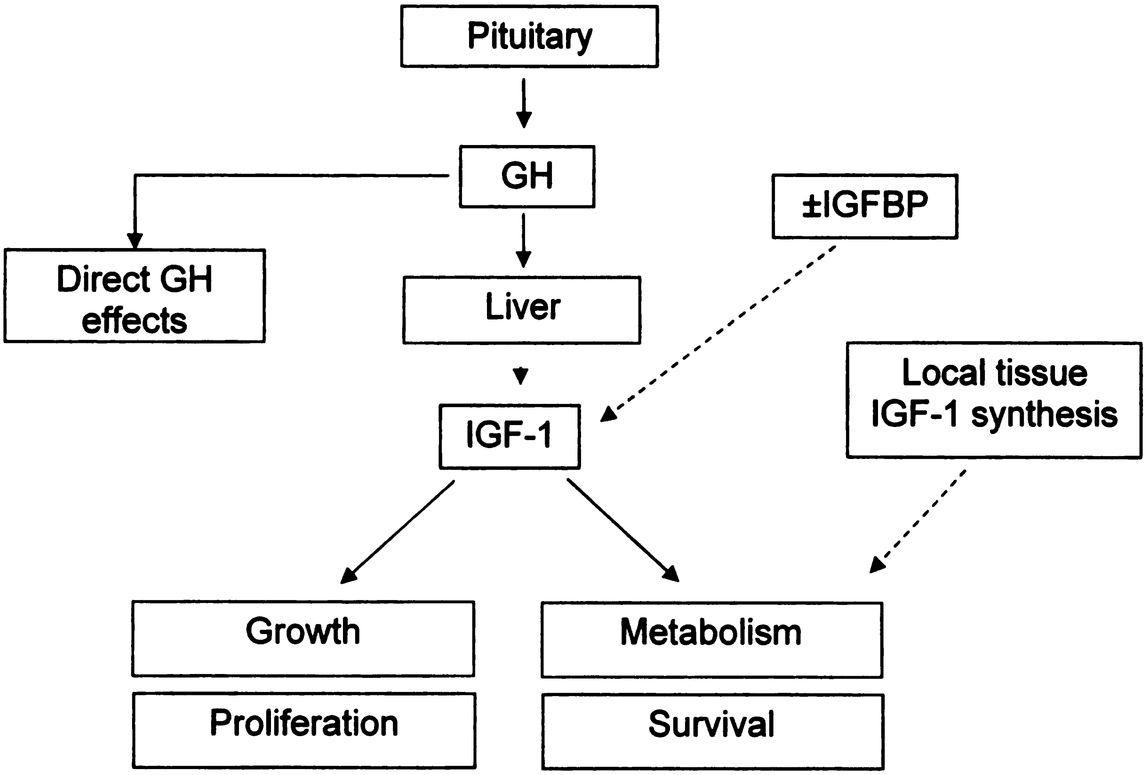

The IGF system is a complex hormone system in the body. It consists of three ligands (IGF-1, IGF-2 and insulin), three receptors (IGF-1 receptor, IGF-2/mannose-6-phosphate receptor and insulin receptor), and six known IGF-binding proteins (IGFBP-1-6). IGF-1 and IGF-2 exert their mitogenic activities via binding to the IGF-1 receptor. The IGF-2/mannose-6-phosphate receptor does not seem to have any effect on IGF-1 signaling but is thought to sequester and remove circulating IGF-2 during fetal development (Kiess et al., 1987; Baker et al., 1993). All of the binding proteins bind to both IGF-1 and IGF-2. Insulin and IGF-1 can weakly bind to the other's receptor.

The IGF-1 and insulin receptors are heterodimeric proteins that possess about 60% overall homology. They both contain an extracellular α-subunit and a membrane-spanning β-subunit that transmits the signal to the intracellular signaling pathways. The α-subunit is made up of two ligand binding sites that are separated by a cysteine-rich domain and two fibronectin III binding domains (Fn0 and Fn1) towards the N-terminus. The extracellular domain of the β-subunit is made up of two fibronectin III-binding domains (Fn1 and Fn2). The intracellular domain contains a juxtamembrane domain close to the plasma membrane, a tyrosine kinase domain that acts as an anchor for intracellular signaling molecules and a C-terminal domain that also anchors signaling molecules. A disulfide bridge between the Fn1 domain on the α-subunit and the Fn2 domain on the β-subunit connects the two proteins. Assembled holoreceptors are connected by disulfide bridges between the Fn0 and Fn1 domains on the α-subunit. While each dimer is capable of binding to the ligand, the holoreceptor forms a binding pocket that increases the affinity of the receptor for the ligand (DeMeyts et al., 2004).

IGF-1 and regulation of the cell cycle

The cell cycle refers to the period in the cell's life when it undergoes cell division. The cell cycle is separated into four different phases: the M (mitosis) phase, the G (gap) 1 phase, the S (DNA synthesis) phase, and the G2 phase. In each phase, the cell performs certain tasks that prepare it for mitosis. Therefore, the tasks that are performed in each phase must be regulated to prevent errors in the creation and transmission of parental DNA to the new cells. Cyclins, cyclin dependent kinases (cdk), and cyclin dependent kinase inhibitors (cdki) act as cell cycle machinery within the cells to promote the accurate progression of cells through the cell cycle. Furthermore, mitogens can direct their signals to regulate the cell cycle machinery, which then regulate progression of the cell through the cell cycle.

IGF-1 exerts its proliferative effects by regulating the cell cycle. In breast cancer cells, IGF-1 promotes passage of the cell through the G1 phase by increasing cyclin D1 transcription and translation via the PI3K/Akt signaling pathway (Dufourny et al., 1997; Muise-Helmericks et al., 1998). Cells from IGF-1-knockout mice display a retarded progression through the G2 phase, suggesting that IGF-1 regulates the passage of cells to the M phase (Adesanya et al., 1999). IGF-1 increases the expression of cyclin A, cyclin B1, and cdk1 in human osteosarcoma cells, genes that are known to regulate passage through the G2 phase (Furlanetto et al., 1994). Furthermore, IGF-1 inhibits expression of the cdki p27 in rat satellite muscle cells and p27 and p21 in cardiomyocytes (Medema et al., 2000; von Harsdorf et al., 1999). However, the effect of IGF-1 on cdki may be cell-specific as IGF-1 increases the mRNA and protein levels of p21 in MCF-7 cells (Lai et al., 2001).

IGF-1 in mammary tissue

IGF-1 increases mammary epithelial cell proliferation in the bovine mammary gland in both *in vivo* and *in vitro* models. Cultured mammary epithelial cells proliferate when exposed to IGF-1 (Collier et al., 1993; Matitashavili et al., 1997). IGF-1 increases DNA content (tritiated thymidine incorporation) compared to untreated cells (Zhao et al., 1992). Mammary explants treated with different doses of IGF-1 increase mammary epithelial cell proliferation in a dose dependent manner as measured by tritiated thymidine incorporation (Baumrucker and Stemberger, 1989). Furthermore, intramammary infusion of IGF-1 increases DNA content per gland and the number of cells undergoing mitosis (Collier et al., 1993; Silva et al., 2005).

The mammary gland produces IGF-1. IGF-1 mRNA and protein have been localized to the stromal elements of the bovine mammary gland (Hauser et al., 1990), ovine mammary gland (Hovey et al., 1998a) and human breast (Yee et al., 1989).

Epithelial cells express IGF-1 mRNA but seem incapable of producing the IGF-1 protein (Campbell et al., 1991), suggesting that IGF-1 is transported from the stromal tissue to the epithelial cells. IGF-1 receptor mRNA was found in the alveolar epithelial cells in bovine mammary glands (Glimm et al., 1992; Purup et al., 1995). In an immortalized bovine mammary epithelial cell line, researchers found that the cells expressed very little IGF-1 (Romagnolo et al., 1994).

IGF binding proteins

While six IGF-1 binding proteins (IGFBP) with high affinity for IGF-1 are known to exist, research on the effects of these proteins in the mammary gland have focused primarily on IGFBP-2, IGFBP-3, and IGFBP-5. IGFBP-3 is a 46-53 kDa protein that acts as the main carrier of circulating IGFs. It is estimated that around 75% of the circulating IGF-1 is transported in the blood bound to IGFBP-3 that forms a 150-kDa complex with the acid labile subunit protein. This binding extends the half life of IGF-1 from between 30 and 90 minutes for the freely circulating IGFs to 12 to 15 hours (Zapf et al., 1986; Guler et al., 1989). IGFPB-3 is synthesized in numerous tissues, including mammary epithelial cells (Cohick and Turner, 1998; Strange et al., 2002), and acts to regulate IGF binding to the IGF-1 receptor. *In vitro* studies utilizing chick fibroblasts show that IGFBP-3 inhibits IGF-1 action when co-cultured with IGF-1 at a 3 to 4-fold molar excess (Blat et al., 1989). In primary bovine mammary epithelial cells, IGFBP-3 inhibited DNA synthesis at equimolar or greater concentrations relative to IGF-1 (Weber et al., 1999). Jones and Clemmons (1995) showed that the IGF-inhibitory effect of IGFBP-3 is due to sequestration of IGF-1 away from its receptor. However, research on IGFBP-1 seems to support an IGF-independent mechanism for inhibition of DNA synthesis by some IGFBP. Proteolysis of a 16-kDa fragment led to inhibition of insulin action in chick embryo fibroblasts and the mitogenic activity of fibroblast growth factor in both wild-type and IGF-1 receptor-knockout cells (Zadeh and Binoux, 1997). Furthermore, endogenous IGFBP-3 from transfected bovine mammary epithelial cells enhanced the mitogenic activity of IGF-1 by as much as 11-fold as compared to mock-transfected controls treated with the same amount of IGF-1 (Grill and Cohick, 2000).

IGFBP-2 is synthesized in many tissues in the bovine, including mammary epithelial cells (Cohick and Turner, 1998; Weber at al., 2000). IGFBP-2 primarily acts as a competitor with the IGF-1 receptor for IGF-1 and IGF-2. Thus, IGFBP-2 inhibits IGF-stimulated DNA synthesis by sequestering IGF-1 away from the IGF-1 receptor (Jones and Clemmons, 1995). IGFBP-2 synthesis from mammary epithelial cells is not altered by the presence of IGF-1 in vitro (Cohick and Turner, 1998; Weber at al., 2000).

IGFBP-5 inhibits IGF-mediated cell proliferation and is associated with involution and apoptosis. Treating osteosarcoma cells with a molar excess of IGFBP-5 inhibited IGF-1 stimulated DNA synthesis (Conover and Kiefer, 1993). IGFBP-5 is highly expressed in both the pubertal and the pregnant murine mammary gland (Wood et al., 2000). In bovine mammary epithelial cells, IGFBP-5 mRNA expression increases during late lactation and tapers off during the dry period (Plath-Gabler et al., 2001). Mice overexpressing IGFBP-5 in the mammary gland show decreased expression of the antiapoptotic bcl-2 and bcl-x proteins and an increase in the expression of caspase-3 (Tonner et al., 2002), thereby implicating IGFBP-5 as a mediator of apoptosis.

Interaction of IGF-1 and other hormones on mammary development

In a series of experiments examining the effects of ovariectomy and GH administration on the local GH/IGF-1 system in the udders of prepubertal heifers, Berry et al. (2003a) found that ovariectomy reduced IGF-1 mRNA expression in the mammary gland and reduced IGF-1 binding to mammary parenchyma microsomes. Administration of estrogen (E) and GH to intact heifers led to an increase in mammary epithelial cell proliferation. While estrogen administration significantly increased mammary development, GH administration alone only tended to increase mammary development ($P < 0.10$). The researchers noted that there was no significant interaction of GH and E. Thus, they suggested that the effect of both hormones on cell proliferation is additive. The effect of ovariectomy on local IGF-1 production is unclear. Berry et al. (2003a) noted that E administration to intact heifers tended to increase IGF-1 mRNA levels in the mammary gland ($P < 0.09$). Furthermore, E administration significantly increased IGF-1 protein content in all of the mammary tissues (Berry et al., 2001). This suggests that estrogen may mediate mammary development through increased synthesis of IGF-1. Estrogen increases IGF-1 expression via the AP-1 enhancer region in the IGF-1 promoter region, thereby supporting the idea that estrogen mediates IGF-1 synthesis (Umyahara et al., 1994).

IGF-1 also interacts with other hormones to affect mammary development. In rodents, epidermal growth factor (EGF) is needed for IGF-1 to affect mammary epithelial cell development in the absence of serum (Imagawa et al., 1986). Both EGF and IGF-1 induce early G1 cyclin expression but IGF-1 also induces late G1 and G2 cyclin expression and is needed by the cells to enter the S phase of the cell cycle (Stull et al., 2002). Bovine mammary epithelial cells cultured with IGF-1 in serum-free media do not require EGF for growth (Shamay et al., 1988). However, when serum is added to the media, IGF-1 and EGF show strong synergism, suggesting that other factors present in serum that are necessary to influence the additive effect of IGF-1 and EGF on bovine mammary epithelial cell proliferation (Shamay et al., 1988).

The extracellular matrix (ECM) affects IGF-1 actions in the mammary gland. Hovey et al. (1998b) showed that murine mammary epithelial cells, when cocultured with a mammary fat pad, showed a 21-fold increase in IGF-1 mediated epithelial cell proliferation as compared to epithelial cells cultured with IGF-1 in the absence of a mammary fat pad. Mammary epithelial cells grown on different ECM proteins show an increase in the number of IGF-1 and EGF receptors (Woodward et al., 2000). Thus, the actions of IGF-1 are influenced by a number of different factors.

Intracellular signaling pathways activated by IGF-1

The binding of IGF-1 to its receptor initiates signal cascades down a number of pathways. Ligands bind to the α-subunit and induce structural changes in the β-subunit that leads to autophosphorylation of specific tyrosine residues in the tyrosine kinase domain of the β-subunit. Upon autophosphorylation, the ligand-bound receptor is internalized via endocytosis which enhances intracellular signaling by IGF-1 (Furlanetto, 1988; Lin et al., 1988). A number of different signaling molecules can then bind to the phosphorylated receptor. Most research has focused on the mitogen-activated protein kinase (MAPK) pathway and the phosphotidylinositol-3 kinase (PI3K) pathways. These pathways are initiated by the insulin related substrates (IRS 1-4) and Shc. Autophosphorylation of the tyrosine residues in the juxtamembrane region of the β-subunit provides an anchor for IRS and Shc to bind. When bound, IRS then can transmit the signal through different pathways via the signaling molecules Fyn, Syp, Nck, and p85. Binding of p85 to IRS leads to activation of phosphoinositol-3' kinase and then the serine/threonine kinase Akt. Akt phosphorylates the proapoptotic molecule Bad, which allows 14-3-3ζ to bind to and inactivate Bad, thereby preventing apoptosis (Butler et al., 1998). Shc binding to the phosphorylated receptor activates the MAPK pathway and, in turn, the Ras-Raf signaling molecules. This pathway leads to the transcription of genes that stimulates cell proliferation. In support of this idea, IGF-1 stimulates MAPK activity in nonmalignant mouse mammary cells (Merlo et al., 1996).

The pathways do not operate independently but interact with each other. Interactions among the pathways allow for signaling to occur if components of one pathway are not available. For example, 14-3-3ε interacts with the mitochondrial version of Raf and inactivates Bad via phosphorylation. IGF-1 may also initiate transcription through the Janus kinase/signal transducer and activator of transcription (JAK/STAT) pathway. Zong et al. (2002) demonstrated that STAT3 is activated by the IGF-1 receptor and that JAK1 or JAK2 is required for IGF-1-induced STAT activation. The STAT family of proteins plays an important role in cellular proliferation and transformation, and STAT3 has been shown to be important in EGF-regulated cell proliferation (Grandis et al., 1988).

The end result of IGF-1 transmitting its signal through numerous pathways is that different cellular mechanisms are influenced so that the cell may proliferate. One such mechanism is the regulation of gene expression. Because IGF-1 transmits its signal through different pathways, it can alter the expression of many genes at a given time. To best capture the full extent of changes in gene expression in genes related to proliferation and cell survival, a method of examining the changes in expression of a large number of genes in a tissue is needed. Microarrays provide the means for examining global gene expression changes.

The gene microarray

The concept of microarray design could be seen in dot blot experiments. Dot blot experiments allowed for simultaneous analysis of multiple recombinant DNA libraries. In dot blot experiments, nucleic acids collected from samples (the targets) are spotted onto a porous support, such as nitrocellulose. Next, nucleic acids of known sequences (the probes) are labeled with fluorescent or radioactive markers and are hybridized to the targets on the porous support. A deviation on this procedure, the reverse dot blot, was created by Saiki et al. (1989) in which the probes were attached to the support. The introduction of impermeable supports, such as glass and polypropylene, allowed for consistent and defined spotting of nucleic acids onto the support and, more importantly, the *in situ* synthesis of probes directly onto the support. The adaptation of ink-jet printing and flow channel technologies provided for economically viable large-scale design and creation of microarrays.

The actual procedure of performing microarray experiments is relatively straightforward and consists of several steps. First, researchers collect messenger ribonucleic acid (mRNA) from the experimental tissues. The mRNA is then amplified into complimentary DNA (cDNA) using one of several commercially available reverse transcriptase kits. The cDNA is then labeled with a fluorescent or radioactive marker and hybridized to the probes on the array. After hybridization, the array is washed and scanned by a laser that is attached to a confocal microscope and a digital camera or is measured for radioactivity levels. Pictures or radiograms are taken of the array and the spots on the images are aligned using a spot alignment program such as Spotfire or GenePix Pro. The data is then log transformed and normalized using a normalization procedure such as LOESS before it can be analyzed for differences in gene expression between treatments. Microarray analysis allows for rapid and cost-effective data collection.

The bovine metabolism (BMET) array was designed to analyze the expression of genes related to metabolism and metabolic regulation, including proliferation, in the dairy cow (Etchebarne, 2005). A list of genes in metabolic and proliferative pathways was extracted from online human genome databases such as the Kyoto Encyclopedia of Genes and Genomes, Swiss-Prot Metabolic Pathway, and the Biocarta website. The human sequences of the genes in this list were then paired for homology to bovine expressed sequence tags using the Basic Local Alignment Search Tool. Highly homologous sequences were found by selecting those tags that had an expectancy value of less than 10^{-35}. A total of 2,360 bovine sequences related to metabolism and proliferation were selected from these search methods for oligonucleotide design. Oligonucleotides of the selected bovine sequences were custom made by the Massachusetts General Hospital Microarray Core Facility and attached to poly-L-lysine coated slides. To reduce the effects of spot position on array and improve the detection of small changes in gene expression, each sequence was spotted 4 times on the array. Furthermore, housekeeping gene sequences and sequences of genes from *Arabidopsis thaliana* were spotted on the array to act as internal controls. Thus, the BMET array will allow us to accurately determine changes in gene expression.

The MAC-T cell line as a model of mammary epithelial cells

To analyze gene expression changes, we need a bovine mammary epithelial cell model that proliferates in response to IGF-1. The MAC-T cell line is an immortalized bovine mammary epithelial cell line retains some epithelial cell characteristics. Mammary epithelial cells from lactating Holstein cows were transfected with the simian virus 40 large-T antigen. The transfected cells demonstrated the cobblestone morphology and a cytokeratin fibril mesh that is characteristic of epithelial cells. Furthermore, upon differentiation the cells reportedly rearrange themselves into lumen-like organoids and express casein proteins (Huynh et al., 1991).

Zavizion et al. (1995) examined the MAC-T cell line as a viable epithelial cell model. They discovered that the MAC-T line was comprised of three different types of mammary epithelial cells, each possessing different characteristics. The researchers subcloned the MAC-T cells into three different clones: CU-1, CU-2, and CU-3. Each subclone possesses different morphologies. CU-1 did not form a "cobblestone" pattern until it reached confluence and required fetal bovine serum (FBS) for growth. CU-3 contained epithelial-like cells but also had much larger, multinucleated cells. Furthermore, the CU-3 subclone did not require FBS for growth. Finally, each subclone exhibited differences in the chromosome arrangements. Zavizion et al. looked for evidence that one or more of these subclones may be myoepithelial in nature. The subclones were devoid of vimentin, α-actinin, and α-smooth muscle actin filaments, indicating that the cells were epithelial and not myoepithelial in nature. Furthermore, the cells did not contract in the presence of $10^{-5}M$ of oxytocin. The researchers concluded that there was some instability in the phenotype of the MAC-T line. While this instability may call into question the validity of the MAC-T line as an adequate mammary epithelial cell model for examining differentiation, I believe that the MAC-T cell line is a viable model to test the effects of IGF-1 on cell proliferation, and to test my hypothesis, it is critical that the cells proliferate in response to IGF-1. Primary cells can undergo senescence, in which they stop proliferating after being passaged too many times (Matitashvili et al, 1997). The MAC-T cell line is a pure population of bovine mammary epithelial cells, albeit with modifications, and, most importantly, MAC-T cells consistently increase proliferation in response to IGF-1.

The MAC-T cell line responds in proliferation to IGF-1 treatments in a manner similar to primary bovine mammary epithelial cells. In primary bovine mammary epithelial cells, the maximal proliferative response using tritiated thymidine incorporation occurs at ~25 ng/mL IGF-1 and is ~3.5 times basal proliferation (Weber et al., 1999). In MAC-T cells, the maximal proliferative response using tritiated thymidine incorporation occurs at 5 to 10 ng/mL IGF-1 and is ~3 times basal proliferation (Silva, 2002; Jacobsen, unpublished results). Therefore, much of the signaling pathways are likely still intact in the MAC-T cells, and MAC-T cells should serve as a good model for my study.

Summary

Mammary development is impaired in heifers fed for high rates of gain. However, IGF-1, a potent mammary epithelial cell mitogen, is increased in the serum of heifers fed for high rates of gain. The binding of IGF-1 to its receptor initiates a signaling cascade that promotes proliferation and cell survival, yet how IGF-1 affects mammary development in heifers is not well understood. A better understanding of the intracellular pathways involved in mediating the mitogenic effects of IGF-1 in bovine mammary epithelial cells may help us understand how nutrition influence mammary development.

My hypothesis is that IGF-1 alters the expression of genes in a manner consistent with proliferation in bovine mammary epithelial cells. Microarray technology allows for rapid determination of changes in overall gene expression. The MAC-T cell line provides an adequate model for looking at IGF-1 effect on bovine mammary epithelial cells. Therefore, my objective was to determine if IGF-1 treatment for 8 and 24 hours alters the expression of genes in the MAC-T bovine mammary epithelial cell line in a manner consistent with increased proliferation.

Materials and Methods

Cell Culture

In my thesis, "experiment" refers to the sets of cultures raised for gene expression analysis at 8 hr and 24 hr on a given day. Experiments were repeated 3 times.

Lyophilized recombinant human IGF-1 (GroPep Pty, Adelaide, Australia) was reconstituted in 2.5 mL of 100 m*M* HCl and then mixed with 2.5 mL of 100 m*M* NaOH. The IGF-1 was separated into 90-µl aliquots and stored at -20°C. Frozen immortalized mammary epithelial (MAC-T) cells were plated at a density of $5x10^3$ cells/cm^2 in 12 T-75 flasks. The MAC-T cell line was chosen as the biological model because it is a homogenous cell population in terms of cell type and stage of differentiation. Homogeneity avoids the phenotypic and genetic variation associated with collecting primary cells from different animals (Mattitashvili et al., 1997). The cells were treated with DMEM-F12 media (GIBCO) and 10% fetal bovine serum (FBS; Invitrogen, Carlesbad, CA) and incubated overnight at 37°C in 5% CO_2. The media was supplemented with 2 ng/mL insulin, 2 ng/mL sodium selenite, 10 µg/mL apo-transferrin, 2 µg/mL soybean trypsin inhibitor, and 2 µg/mL glutathione (Sigma). After incubating for 24 hours, the cells were washed with phosphate buffered saline (PBS) and were treated with serum-free medium, which consisted of DMEM-F12 and 750 µg/ml bovine serum albumin (BSA; Invitrogen) and incubated for another 48 hours.

Next, the cells were washed twice with PBS and treated with either 0 ng/mL or 100 ng/mL IGF-1 for 8 hours. The 100 ng/mL dose was chosen based upon the IGF-1 doses-response data from Silva et al. (2002). Silva showed a maximal proliferative response of MAC-T cell to 100 ng/mL IGF-1. To verify the proliferative effect of this dose on cell proliferation, MAC-T cells were treated with either 100 ng/mL or a serum-free medium control for 18 hr. After 18 hr, the cells were exposed to tritiated thymidine and proliferation was estimated by measuring the amount of tritiated thymidine uptake. IGF-1 increased tritiated thymidine uptake by over 3-fold, demonstrating that 100 ng/mL of IGF-1 has a proliferative effect on MAC-T cells. The IGF-1 effect for this project was validated by estimation of confluency by two observers blinded to treatment at 24 hours after IGF-1 administration.

Figure 3. Proliferative effect of 100 ng/mL IGF-1 on MAC-T cells after 18 hr of IGF-1 treatment.

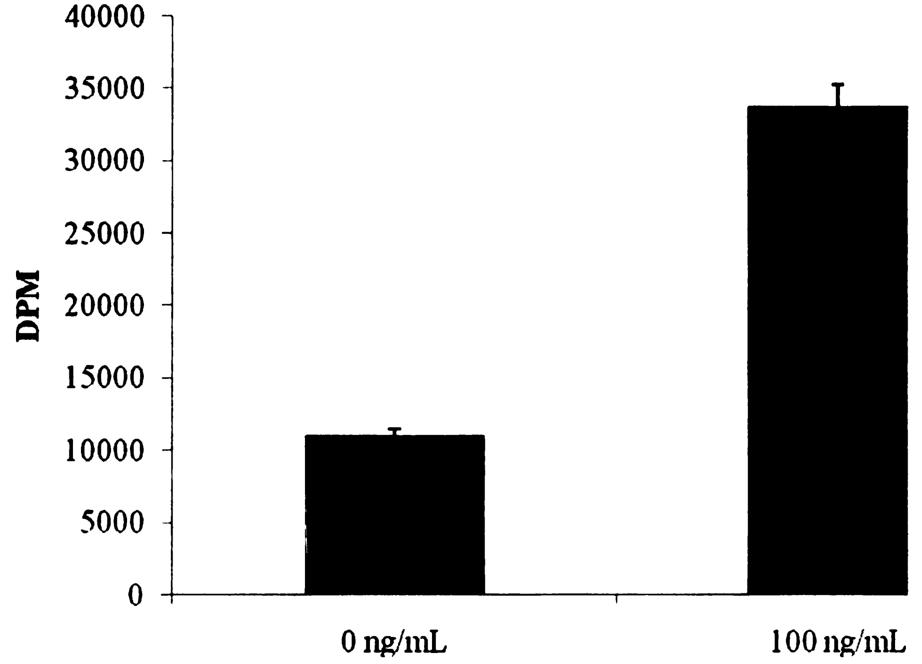

RNA extraction

The cells were washed with PBS before RNA isolation. RNA was extracted by the Trizol method (Invitrogen). After washing the cells one time with PBS, cells were scraped into 2 mL of Trizol per flask and they were incubated at room temperature for 5 min. Next, 200 μL of chloroform per ml of Trizol was added and the lysate was shaken vigorously for 10 seconds. After incubating at room temperature for 3 min, the lysate was centrifuged at 10,500 rpm for 15 min and the aqueous phase was mixed with 500 µL isopropanol. After incubating for 10 min at room temperature, the RNA was centrifuged at 10,500 rpm for 10 min. The isopropanol was removed and the RNA pellet was washed with 1 mL of 75% ethanol and centrifuged at 8500 rpm for 5 min. The ethanol was removed and the pellet was allowed to dry at room temperature for 10 min. The pellet was resuspended in 14.8 µL of RNase-free water and incubated in a 37°C water bath for 5 min. Next, the RNA from three flasks was combined to form a total volume of 89 µL (14.8 mL water per mL Trizol from 2 mL Trizol per flask from 3 flasks). Then, 10 µL of 10X RQ DNase buffer and 1 µL of RQ1 DNase (1U/mL, Ambion) were added to each RNA sample and the samples were incubated at 37°C for 30 min. The RNA was mixed with 100 µL of a 25:24:1 phenol:chloroform:isoamyl alcohol solution (pH 4.0, Invitrogen). The RNA was centrifuged at 14,000 rpm for 2 min and the aqueous phase was mixed with 9 µL of 3*M* sodium acetate (Ambion) and 250 µL ethanol. The RNA was precipitated overnight at -20°C. After precipitation, the RNA was centrifuged at 14,000 rpm for 15 min and washed with 500 µL of cold 75% ethanol. The RNA was centrifuged at 14,000 rpm for 10 min and the ethanol was removed. The pellet was allowed to dry in a chemical hood for 15 min and then was resuspended in 25 µL of nuclease-free water. After incubated at 55°C for 10 min, the RNA was immediately transferred to ice. The concentration and quality were determined in the Center for Animal Functional Genomics using a NanoDrop ND-1000 spectrophotometer and an Agilent 2100 Bioanalyzer. Samples were then stored at -80°C until use for hybridizations.

Microarray hybridization

Complementary DNA (cDNA) was transcribed from mRNA and dye-coupled using the SuperScript Indirect cDNA Labeling Core Kit and the cDNA Labeling Purification Module (Invitrogen). First, 10 μg of RNA was mixed with 5 μg of anchored oligo(dT) primers. DEPC-treated water was added to bring the volume to 18 μL. This mix was incubated at 70°C for 5 min in a thermocycler (GeneAmp PCR System 9700). A "master mix" consisting of 6 μL 5X first-strand buffer, 1.5 μL 10 m*M* dNTP mix, 1.5 μL DTT, 1 μL RNaseOUT, and 2 μL SuperScript III per sample was added to each sample and the reaction was continued at 46°C for 3 hr. Then, 15 μL of 1N NaOH was added to each reaction, and the reactions were continued at 70°C for 10 min. The NaOH was neutralized with an equal amount of 1N HCl at the end of the amplification.

Next, 20 μL of 3 *M* sodium acetate was mixed into each sample, and 500 μL of the kit's loading buffer were added to each sample. The cDNA was pipetted into a S.N.A.P. column™ (Invitrogen) and centrifuged at 12,000 x g for 1 min. A loading buffer and a washing buffer from the Purification Module kit were mixed with 10 mL isopropanol and 25 mL ethanol, respectively. The cDNA, which was trapped in the column, was washed twice with 700 μL washing buffer and centrifuged at 12,000 x g for 1 min. The cDNA was eluted with two 50-μL washes of DEPC-treated water, and the concentration was determined on the NanoDrop ND-1000 spectrophotometer. The cDNA was then mixed with 10 μL of 3*M* sodium acetate and 2 μL of 20 mg/mL glycogen and precipitated overnight in -20°C.

The next day, the cDNA was centrifuged at 12,000 x g for 20 min and was washed in 75% ethanol. The cDNA was then spun at 14,000 x g for 5 min and then dried at room temperature for 12 min. The cDNA was resuspended in 5 µL of 2X coupling buffer. The fluorescent dyes Cy3 and Cy5 (Cy™Dye Post-labeling Reactive Dye Pack, Amersham Biosciences) were mixed in 11 µL of dimethyl sulfoxide (DMSO). 5 µL of the dye/DMSO mix was mixed into each sample. The samples were then covered in foil and were incubated in the dark at room temperature for 2 hr. The dye-coupling reaction was halted with 20 µL of 3*M* sodium acetate and the dye-coupled cDNA was mixed in 500 µL of washing buffer from the kit. The cDNA was loaded onto a S.N.A.P. column and centrifuged at 14,000 x g for 1 min. The cDNA was washed with 700 µL of washing buffer and centrifuged at 14,000 x g for 1 min twice per sample. The dye-coupled cDNA was eluted by centrifuging 50 µL of DEPC-treated water through the column at 14,000 x g for 1 min. The concentrations of dye-coupled cDNA were measured using the NanoDrop ND-1000 spectrophotometer. The Cy3 dye-coupled samples were mixed with their respective Cy5 dye-coupled samples in one-1.5 mL Eppendorf tube and the combined samples were centrifuged at 12,000 x g for 12 min through a Microcon filter (Millipore). Next, 20 µL of SlideHybe #1 (Ambion) was added to the Microcon filter and the filter placed upside-down into a clean Microcon tube. The combined sample was centrifuged at 2500 rpm for 3 min. The probe was then brought to a volume of 110 µL. The samples were then stored in a 68°C water bath until arrays were prepared for the samples.

The samples were hybridized onto 2 BMET arrays per time. A dye-swap design was used for the microarray experiment to remove the preferential binding of dyes to certain transcripts. The arrays were loaded into a Genomic Solutions HybStation and the probe was allowed to hybridize to the array for 18 hr. After hybridization, the arrays were washed three times in 0.06X SSC (Ambion) and were scanned on an Axon 4000B Scanner and the Agilent Scanner. Gains were adjusted such that the intensities of each dye were approximately 1:1. Spots were aligned using the GenePix Pro software before analysis.

Quantitative RT-PCR

Genes of interest were validated by quantitative RT-PCR using the SuperScript II reverse transcriptase procedure. The genes of interest were selected due to their relation to proliferation. To accurately validate the microarray data, I selected some genes that were significantly upregulated, some that were significantly downregulated, and some that were not significantly altered according to the microarray data. For genes to be considered significantly altered (either upregulated or downregulated), they had to pass two criteria: 1) they were expressed at $P < 0.05$, and 2) they were altered at a ratio of >1.2 or <0.8. This removes all genes that show small changes in expression, which may be attributed to random noise.

All products came from Invitrogen unless otherwise noted. First, cDNA was synthesized from each RNA sample. I mixed 2 μg of RNA per sample with 1 μL (100 μ*M*) of oligo $dT_{12\text{-}18}$ primers, and the reaction was brought to 10 μL with RNase-free water in a labeled PCR tube. The samples were then loaded into a GeneAmp PCR System 9700 and were heated to 70°C for 5 min and then 20°C for 5 min. During this time, a 'master mix' was prepared on ice for each reaction in which 4 μL 5X First Strand Buffer, 2 μL 0.1 *M* DTT, 1 μL SuperScript II RNase H reverse transcriptase, 2 μL RNase-free water, and 1 μL 10m*M* dNTP mix were combined for a total of 10 μL for each sample. After the 20°C incubation, 10 μL of the master mix was added to each reaction and the samples were heated to 42°C for 60 min and 70°C for 5 min. The samples were cooled to 37°C, and 0.5 μL of RNase H (10U/μL) was added to each sample. The samples were kept heated at 37 °C for 20 min, after which 0.2 μL of 0.5 *M* EDTA (pH 8.0) was mixed into each sample. Next, 5 μL of 3 *M* sodium acetate (Invitrogen), 25 μL of RNase-free water, and 125 μL of ice-cold EtOH was added to each sample and the cDNA precipitated overnight at -20°C. After precipitation, the cDNA was spun at 14,000 x *g* for 20 min and washed with 250 μL of cold 75% EtOH. The cDNA was spun at 14,000 x *g* for 6 min and the EtOH was removed. The pellet air-dried for 15 min and was reconstituted in 50 μL of RNase-free water. The cDNA concentration was measured using the NanoDrop ND-1000 spectrophotometer.

Quantitative real-time RT-PCR (qRT-PCR) was carried out using the SYBR Green Master Mix from Applied Biosystems. Primer sets for approximately 20 genes were tested at various concentrations for successful amplification of my samples. For those primer sets that were successfully amplified, their amplification efficiencies were measured for similarity with glyceraldehyde-3-phosphate dehydrogenase (GAPDH). The primer sets I used are shown in table 1 on page 31. Primers were designed by Primer Express (v.) except for RPS9, RPS15, and UTX, which were taken from Bionaz and Loor (2007).

The RT-PCR reactions were run on two separate plates with three genes plus GAPDH on each plate. All 6 treatment samples were performed in duplicate. First, 20 μg (2 μL of 10ng/μL) of sample cDNA, 3 μL of 5 μ*M* primer mix, 7.5 μL RNase-free water, and 12.5 μL SYBR Green Master Mix (Applied Bioscience) were mixed on ice for a total reaction volume of 25 μL. The RT-PCR reaction were carried out in a ABI Prism

7500 RT-PCR System using the following protocol: 50°C for 2 minutes, 95°C for 10 min, 41 cycles of 95°C for 15 seconds and 60°C for 1 min, and 95°C for 15 seconds and cooled to room temperature.

Table 1. Quantitative RT-PCR primer sets.

Accession #	Symbol	Primers set	Melting Temp (^{0}C)	Product length
XM_602780	SLC39A6	F – GCACTTACTGCAGGCTTGTCAT R - CGGCTACATCCATGGTCACTAG	79	92
XM_581382	IRS1	F – TGCGGCCACTCAGAGAACTT R - CCAGGATTGTCTCGTGCATGT	85	124
NM_174000.2	CALR	F - CCGTTTACTTTAAGGAGCAGTTTCTG R - TTGTGCTTGGATTCGATCCA	82	70
NM_174308.1	EDNR1A	F -ATGGACACGAACCGATGTGA R - GGTTGCCAAGTTAATACCGATGT	77	72
NM_174313.2	FABP3	F - CCACAGCAGATGACAGGAAAGTC R - CTGCACGTGGACAAGTTTGC	82	68
NM_175801.1	FST	F - TCCCTTGTAAAGAAACGTGTGAGA R - TCGCCCTCGTCCTTGTCA	79	67
BF606842	HSPA5	F - AAGATGTTCGGAAGGACAACAGA R - GCCCGTTTGGCCTTTTCTAC	82	67
AB072368.1	HSPCA	F - CACCGGCATTGGGATGA R - CCGGACTTGGCGATGGT	82	63
NM_174130.2	ODC1	F - CGCATTGTTGAGCGCTGTA R - CATGTTCTCAAAGAGCATCCAATC	80	66
NM_174217.1	VIL2	F - GCAGCTTTTTGATCAGGTGGTT R - TCCACATACTGGAGGCCAAAGT	75	90
Not Available	18S	F – GAGAAACGGCTACCACATCCA R - GACACTCAGCTAAGAGCATCGA	Not Available	Not Available
Not Available	B-actin	F – CGCCATGGATGATGATATTGC R - AAGCCGGCCTTGCACAT	Not Available	Not Available
DT860044	RPS9	F – CCTCGACCAAGAGCTGAAG R – CCTCCAGACCTCACGTTTGTTC	Not Available	54
XM585783	RPS15	F – GCAGCTTATGAGCAAGGTCGT R - GCTCATCAGCAGATAGCGCTT	Not Available	151
BQ676558	UTX	F – TGTGGCCCTTGGATATGGTT R - GGYYGYCGCTGAGCTCTGTG	Not Available	110
Not Available	GAPDH	F – GCATCGTGGAGGGACTTATGGA R - GGGCCATCCACAGTCTTCTG	Not Available	Not Available

Data Analyses

Differences in cell confluencies between treatments were analyzed using a two-tailed t-test. Median intensities of microarray spots were log-transformed (base-2) and the microarray data was normalized by the LOESS procedure. The microarray data collected from both arrays was analyzed utilizing two mixed linear models, as outlined by Wolfinger et al. (2001). First, differences across all microarrays were standardized using the following model,

$$y_{ijk} = \mu + dye_i + array_j + dye * array_{ij} + block(array)_{jk} + dye * block(array)_{ijk} + \varepsilon_{ijk}$$

Where dye represented the fixed effect and dye*array, block(array), and dye*block(array) represented the random effects for gene i, dye j, array k, and block l.

In the second model, residuals for each gene were calculated by subtracting fitted values obtained from the first model from the observed intensities. Differences in individual gene intensities were analyzed by the following model,

$$r_{ikjlmno} = \mu_i + treatment_m + scanner_n + culture_o + treatment * culture_{mo}$$
$$+ treatment * scanner * culture_{mno} + \varepsilon_{ijkl}$$

Where treatment and scanner represent the fixed effects and culture, treatment*culture, and treatment*scanner*culture represent the random effects of *treatment m, scanner n and culture o*. The data was analyzed using the PROC MIXED procedure of SAS (v. 9.0) using both the Type III Sums of Squares method.

Data for the quantitative RT-PCR experiments was analyzed using the $2^{-\Delta\Delta Ct}$ method proposed by Livak and Schmittgen (2001). The cycles-to-threshold (Ct) values for 18S for each replicate in each sample was subtracted from the Ct values for the genes of interest for each replicate in each sample to obtain the delta Ct values. Independent ttests were performed on the delta Ct values to determine differences in gene expression due to IGF-1 treatment. Because I was verifying the fold-change directions, I analyzed the genes shown to be statistically significant on the microarray data using a one-tailed t-test. I used a two-tailed t-test on the non-significantly expressed genes. The fold-change values for the quantitative RT-PCR experiment were calculated using the following equation:

$$\text{Fold-change} = 2^{(-(\text{gene Ct value} - \text{18S Ct value})-(\text{average 0 ng/}\mu\text{l gene Ct value} - \text{average 0 ng/}\mu\text{l 18S Ct value}))}$$

Results

Cell Confluency Results

I verified the biological effect of IGF-1 on bovine mammary epithelial cells by estimating cell confluencies after treating the cells with IGF-1 for 24 hours in separate flasks. The results are shown in figure 4. IGF-1 treatment for 24 hr increased cell confluencies by 40% as compared to control cells that were not treated with IGF-1 ($P < 0.05$). Furthermore, IGF-1 tended to increase cell confluencies at 8 hr by 20% ($P = 0.06$).

Figure 4. Average cell confluencies at 8 and 24 hours. Error bars are expressed as SEM.

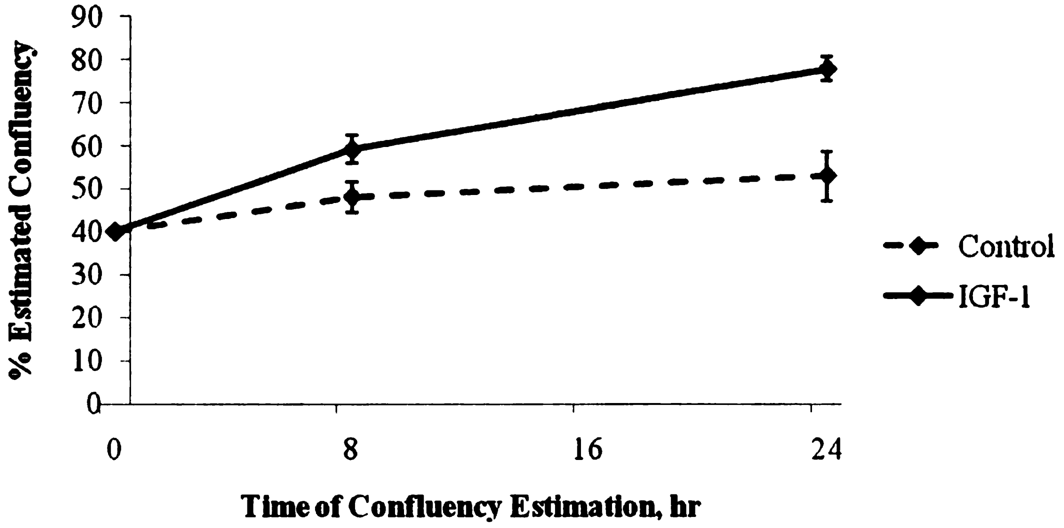

Microarray results

To determine if IGF-1 treatment altered global gene expression, the histograms of the P-values of treatment comparisons for each gene were examined in both the 8 hr and the 24 hr microarray data, as shown in figure 5. These histograms should not show any differences in bar heights if IGF-1 treatment did not affect gene expression. However, the large frequency of genes that were altered at average P-value < 0.05 showed that IGF-1 altered the expression of genes in MAC-T cells at 8 hr and 24 hr of treatment.

Figure 5. P-value distribution histogram of 8 hr 24 hr microarray data.

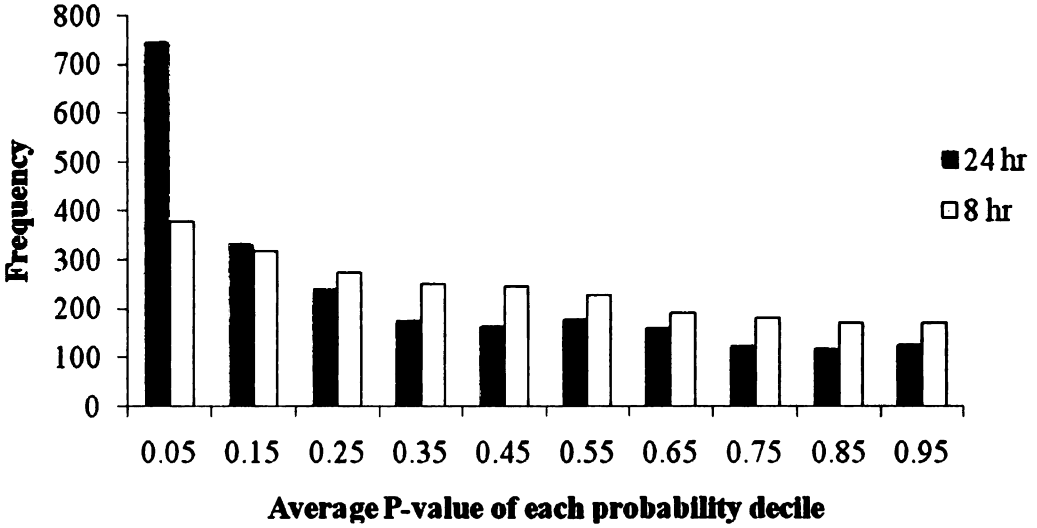

Genes that showed fold-changes in expression of either greater than 1.2 or less than 0.8 due to IGF-1 and had $P < 0.05$ were deemed significantly altered by IGF-1. Table 2 shows the number of upregulated and downregulated genes at 8 hr and 24 hr of treatment.

Table 2. Number of genes altered by IGF-1 at $P < 0.05$.

	8 hr	24 hr
Upregulated > 20%	70	139
Downregulated > 20%	19	45
Total	89	184

These genes were then organized into groups based upon their function as defined by the KEGG pathway and Gene Ontology function. Table 3 shows the functional categories of genes significantly altered by IGF-1. IGF-1 treatment for 24 hr altered a greater percentage of transcribed genes across most categories than treatment for 8 hr. However, a greater percentage of coagulation factor genes (16.7%) and DNA replication and repair genes (16.3%) were altered and also upregulated at 8 hr than at 24 hr (12.5%

respectively). A greater percentage of genes were upregulated in both of these categories at 8 hr than at 24 hr. IGF-1 also downregulated the transcription of a higher percentage of cell signaling (5.1%) genes at 8 hr than at 24 hr (3.1%).

Table 3. Functional categories of genes whose expression was altered by IGF-1 treatment for 8 hr and 24 hr.

		8 hr			24 hr		
Function	**total number on array**	**% upreg of total**	**% downreg of total**	**% altered of total**	**% upreg of total**	**% downreg of total**	**% altered of total**
Carbohydrate Metabolism	113	1.8	0.9	2.7	9.7	6.2	15.9
Cell Cycle and Death	259	0.8	0.0	0.8	1.9	0.8	2.7
Cell signaling	98	10.2	5.1	15.3	15.3	3.1	18.4
Cell Structure and Extracellular Matrix	44	9.1	9.1	18.2	34.1	20.5	54.5
Coagulation Factors	24	16.7	0.0	16.7	8.3	4.2	12.5
DNA Replication and Repair	49	16.3	0.0	16.3	6.1	2.0	8.2
Energy Metabolism	51	21.6	9.8	31.4	21.6	15.7	37.3
Folate Metabolism	22	0.0	0.0	0.0	31.8	0.0	31.8
Glycan Metabolism	38	5.3	5.3	10.5	26.3	10.5	36.8
Lipid Metabolism	198	2.0	0.0	2.0	4.0	2.0	6.1
Protein Synthesis and Metabolism	187	4.8	0.0	4.8	10.2	1.6	11.8
Purine and Pyrimidine Metabolism	96	0.0	0.0	0.0	4.2	0.0	4.2
Signal Transduction	252	2.0	0.4	2.4	4.8	0.4	5.2
Transcription	236	0.0	0.0	0.0	1.3	0.0	1.3
Transport	69	8.7	0.0	8.7	8.7	2.9	11.6
Unknown	624	0.5	0.2	1.7	1.3	0.0	1.3

IGF-1 increases proliferation in mammary epithelial cells, yet there are different mechanisms by which it promotes cell proliferation. We examined changes in the expressions of genes related to proliferation and survival to see if IGF-1 regulates cell proliferation through gene expression. The results can be seen in tables 3 and 4. IGF-1 altered the expression of genes related to the cell cycle and polyamine synthesis at both 8 and 24 hours of treatment. IGF-1 also altered the expression of intracellular signaling genes that are related to proliferation, particularly genes related to the mitogen-activated protein kinase (MAPK) pathway and the Wnt signaling pathway. Furthermore, evidence of IGF-1 signaling through the Janus kinase – signal transducer and activator of transcription (JAK-STAT) pathway could be seen by the downregulation of protein inhibitor of activated STAT 1 (PIAS1) at 8 hours.

Table 4. Proliferation and survival-related genes whose expression was regulated by IGF-1 at 8 hr or 24 hr.

		8 hr			24 hr		
Gene Name	**Symbol**	**Fold-change**	**P-values**	**FDR**	**Fold-change**	**P-values**	**FDR**
Cell cycle							
CDC6 cell division cycle 6 homolog (S. cerevisiae)	CDC6	1.85	0.03	0.30	1.58	0.02	0.11
cyclin E1	CCNE1	1.37	0.03	0.31	1.31	0.04	0.14
cyclin-dependent kinase inhibitor 2B	CDKN2B	0.89	0.39	0.52	0.77	0.01	0.09
Cell signaling							
epidermal growth factor	EGF	1.44	<0.01	0.20	1.34	0.10	0.18
fatty acid binding protein 3, muscle and heart (mammary-derived growth inhibitor)	FABP3	2.13	<0.01	0.26	1.95	<0.01	0.08
insulin-like growth factor binding protein 2, 36kDa	IGFBP2	1.00	0.94	0.66	0.78	0.02	0.11
insulin-like growth factor binding protein 3	IGFBP3	1.40	0.03	0.31	1.42	0.01	0.08
Stress							
heat shock 70kDa protein 5 (glucose-regulated protein, 78kDa)	HSPA5	1.30	0.09	0.40	1.33	<0.01	0.05
heat shock 90kDa protein 1, alpha	HSPCA	1.33	0.18	0.45	1.36	0.03	0.13
Polyamine synthesis							
ornithine decarboxylase 1	ODC1	1.60	<0.01	0.26	1.47	0.01	0.10
spermidine synthase	SRM	1.47	0.10	0.42	1.36	0.02	0.12
Signal transduction							
FOS-like antigen 1	FOSL1	1.38	0.04	0.34	1.41	0.01	0.09
insulin receptor substrate 1	IRS1	0.87	0.40	0.52	0.76	0.01	0.10

Table 4 (continued).

		8 hr			24 hr		
Gene Name	**Symbol**	**Fold-change**	**P-values**	**FDR**	**Fold-change**	**P-values**	**FDR**
lymphoid enhancer-binding factor 1	LEF1	0.77	0.03	0.29	0.83	0.00	0.05
mitogen-activated protein kinase 4	MAPK4	0.95	0.21	0.46	0.74	<0.01	0.08
mitogen-activated protein kinase 6	MAPK6	0.92	0.86	0.64	1.29	0.02	0.11
mitogen-activated protein kinase kinase kinase 7 interacting protein 2	MAP3K7IP2	0.83	0.38	0.51	1.22	0.05	0.15
mitogen-activated protein kinase-activated protein kinase 3	MAPKAPK3	1.23	0.05	0.36	1.25	0.03	0.12
protein inhibitor of activated STAT, 1	PIAS1	0.73	0.04	0.34	0.95	0.27	0.29
protein tyrosine phosphatase, receptor type, R	PTPRR	1.38	0.01	0.27	0.88	0.81	0.52

Samples from two different experiments were used for one set of 8 hr arrays. To determine if this influenced the results, the regression of the differences in residuals of all genes that were expressed at $P < 0.1$ between all three array sets were examined. This significance level was chosen to remove all genes that showed very little differences in dye intensities. As show in Table 5 on page 41, the array sets were strongly and positively correlated. Experiments 1 and 2 represent those arrays sets that had samples within an experiment. Experiment 3 had samples from different experiments. The correlations were highly significant, thereby suggesting that the samples from two different experiments did not affect the 8 hr microarray data.

Table 5. Regression and correlation values of all genes expressed at $P < 0.1$ between the 8 hr arrays

Comparison	R-squared	Correlation	*P*-value
Exp 2 vs Exp 1	0.60	0.77	<0.001
Exp 2 vs Exp 3	0.60	0.77	<0.001
Exp 1 vs Exp 3	0.59	0.73	<0.001

The full lists of differentially expressed genes are found in the appendices. Appendix B lists the genes altered after 24 hr IGF-1 treatment and Appendix C lists the genes altered after 8 hr IGF-1 treatment.

Quantitative RT-PCR results

Quantitative RT-PCR was used to validate significant gene expression changes as reported by the microarray data analysis. A suitable housekeeping gene was needed to accurately analyze the RT-PCR data using the ΔΔCt method. The fold-changes in the expressions of 6 potential housekeeping genes were measured across all experiments. The results can be seen in figure 6. UTX, RPS15, and β-actin were significantly altered by IGF-1 treatment at 24 hr. Of the 3 candidate genes remaining, GAPDH was chosen because it was not significantly altered by IGF-1 and others have used it as a housekeeping gene in MAC-T cells (Smith and Sheffield, 2002).

Figure 6. Quantitative RT-PCR results of candidate housekeeping genes in cells treated with IGF-1 for 24 hr.

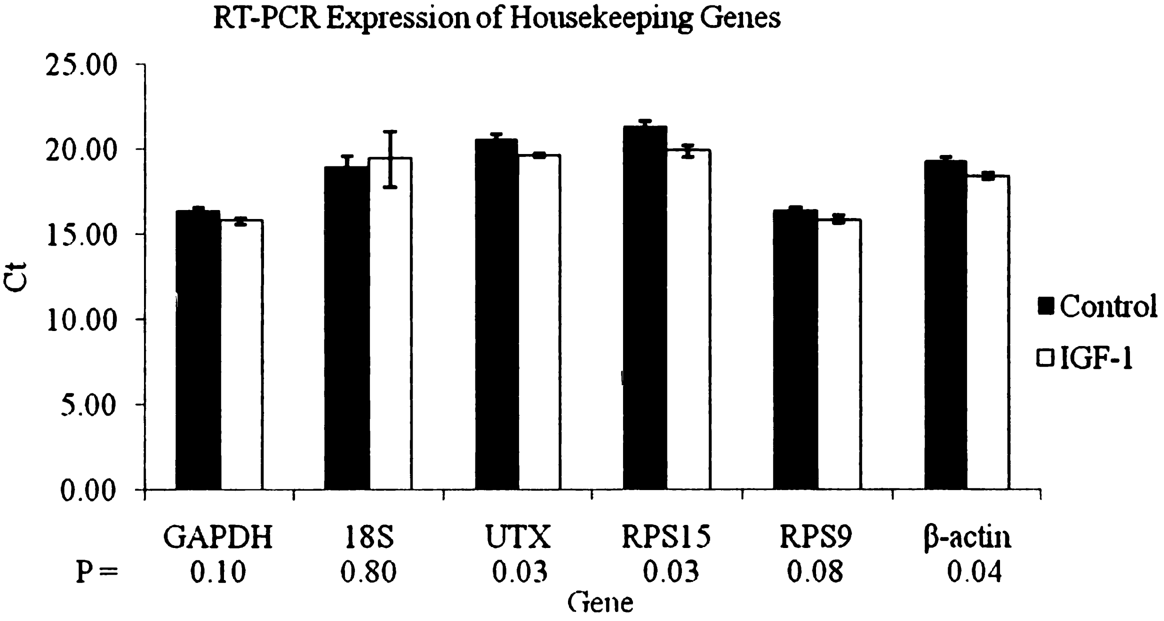

The expression levels of ten genes were analyzed using quantitative real-time RT-PCR to verify the array results. These genes were selected because they were involved in cell proliferation and were either upregulated, downregulated, or not regulated ($P < 0.05$)

by IGF-1 treatment. The microarray and qRT-PCR results for each gene are shown in table 6. Quantitative RT-PCR confirmed the upregulation of only 2 genes (FABP3 and ODC1) at *P* < 0.05 out of the 5 that were upregulated in the microarray analysis. The qRT-PCR fold-change values for each gene were correlated to the microarray fold-change values for that same gene to determine if the RT-PCR fold-change values were similar to the microarray fold-change values. For 7 of the 10 genes, the correlations between the microarray fold-change values and the qRT-PCR fold-change values were positive. For the other 3 genes, there was no correlation.

Table 6. Fold-change values from microarray analysis and qRT-PCR for the validated genes.

		Microarray		**RT-PCR**		
Gene Name	**Gene Symbol**	**fold-change**	***P*-value**	**fold-change**	***P*-value**	**Correlation**
fatty acid binding protein 3, muscle and heart (mammary-derived growth inhibitor)	FABP3	1.95	<0.01	2.06	<0.01[1]	0.74
endothelin receptor type A	EDNRA	1.47	0.01	1.58	0.06[1]	-0.08
ornithine decarboxylase 1	ODC1	1.47	0.01	1.24	0.04[1]	0.86
heat shock 90kDa protein 1, alpha	HSPCA	1.36	0.03	1.32	0.14[1]	0.76
heat shock 70kDa protein 5 (glucose-regulated protein, 78kDa)	HSPA5	1.33	<0.01	1.61	0.06[1]	0.71
calreticulin	CALR	1.19	0.07	2.00	0.22[2]	0.85
villin 2 (ezrin)	VIL2	0.98	0.61	0.92	0.58[2]	0.37
follistatin	FST	0.88	0.08	0.80	0.06[2]	0.44
insulin receptor substrate 1	IRS1	0.76	0.01	0.93	0.40[1]	-0.004
solute carrier family 39 (zinc transporter), member 6	SLC39A6	0.74	<0.01	1.01	0.48[1]	-0.05

1 = one-tailed t-test
2 = two-tailed t-test

Discussion of Results

When mammary epithelial cells are exposed to IGF-1, they initiate cell-cycle progression and activate antiapoptotic mechanisms to promote proliferation. My hypothesis is that IGF-1 alters the expression of genes in a manner consistent with increased proliferation in bovine mammary epithelial cells. The results suggest that my hypothesis is correct. The qRT-PCR results confirmed the expression levels of 9 of our 10 genes of interest, although the statistical significance was the same for only 6 of those genes. We still need to determine which analysis is biologically accurate.

My microarray data shows that IGF-1 altered the expression of genes regulating proliferation and cell cycle. I found that IGF-1 increased the expression of ornithine decarboxylase (ODC1) and spermidine synthase (SRM), enzymes involved in polyamine synthesis. ODC1 converts ornithine to putrecine via decarboxylation and is the rate-limiting step in polyamine synthesis. SRM catalyzes the conversion of putrecine to spermidine in a similar fashion. Proliferating cells require polyamines to continue DNA elongation during the S phase (Oredsson, 2003). However, the type of polyamines required during the different phases of the cell cycle varies. Putrecine levels are doubled during the S phase and during the S/G2 transition, while spermine levels double during the G1 phase (Fredlund et al., 1995). Polyamines are regulated in conjunction with the cell cycle. ODC1 synthesis and activity is cell-cycle specific. In Chinese hamster ovary cells that were made to proliferate synchronously during the cell cycle, ODC1 activity was shown to increase at the G1/S transition and again at the S/G2 transition (Oredsson, 2003). Furthermore, ODC mRNA levels were increased during the G1/S transition but not the S/G2 transition. Blocking ODC1 activity with a-difluromethylornithine led to a cessation of cell proliferation and an increase of cells accumulating at the G1 phase (Oredsson, 2003). Inhibition of SRM activity in chick embryo fibroblasts also blocks DNA synthesis (Caruso et al., 1992). IGF-1 treatment for 24 hr increased ODC1 mRNA expression in breast cancer cells by 3.5-fold (Huber and Poulin, 1996). Therefore, my results suggested that IGF-1 promotes progression of proliferating mammary epithelial cells through the cell cycle by upregulating of ODC1 and SRM expression. ODC1 and SRM then increase polyamine synthesis, thereby promoting DNA synthesis.

IGF-1 also increased the expression of the heat-shock proteins HSPCA and HSPA5 in my study. The expression of the chaperone heat-shock protein 90 (HSPCA) is increased by a number of growth factors, including IGF-1, just before DNA synthesis occurs (Jerome et al., 1991). However, HSPCA appears to have a buffering function on IGF-1 signaling. Blocking HSPCA leads to an amplification of Akt activation, increased p38 activation and an increased duration of ERK1/2 activation (Meares et al., 2004). Therefore, in our MAC-T model, IGF-1 might have increased the expression of HSPCA as a safeguard against overactivity of the proliferative signal. Heat-shock 70kDa protein 5 (HSPA5), an endoplasmic reticulum-localized chaperone protein, blocks the proapoptotic activities of caspase 7 in cells challenged with topoisomerase inhibitors, thereby promoting cell survival (Reddy et al., 2003).

In my study, IGF-1 increased the expression of cyclin E1 and decreased the expression of cyclin-dependent kinase inhibitor 2B (p15, also known as INK4B), genes directly associated with the cell cycle. Cyclin E1 regulates the passage of the cell through the G1/S transition and is required for the initiation of DNA replication (Harper and Brooks, 2005). Mouse mammary explants exposed to IGF-1 showed an increase in cyclin E mRNA levels (Stull et al. 2002). The cyclin-dependent kinase inhibitor p15 is part of the INK4 family of inhibitors. These bind specifically to cyclin D/cdk complexes and inhibit their actions, thereby allowing the cell to begin the S-phase of the cell cycle. Based upon the microarray data, IGF-1 appears to be promoting passage of the cells through the G1/S transition and the S-phase of the cell cycle by increasing the expression of cyclin E1 and decreasing the expression of p15.

The expression of two parts of the endothelin signaling system, endothelin 1 (EDN1) and the endothelin receptor type 1 alpha (EDNRA), were regulated by IGF-1. Endothelin 1 increase cell proliferation and DNA synthesis in many different systems (Battistini et al., 1993). Our results show that EDN1 expression is downregulated by IGF-1. This is supported by the findings that EDN1 expression is increased in the aortas of liver-specific IGF-1-knockout rats (Tivesten et al., 2002). However, IGF-1 increased EDN1 expression in cultured chondrocytes (Messai et al., 2000), thereby suggesting that the effect of IGF-1 on EDN1 expression is system specific. Furthermore, our results show that EDNRA expression was increased by IGF-1. Similar results have been found in vascular smooth muscle cells (Kwok et al., 2005). The net result of IGF-1 promoting the expression of the receptor and not the ligand is that IGF-1 would make the cell more responsive to endothelin signaling from other cells. The presence of more endothelin receptors on the cell will increase endothelin signaling to the epithelial cell. Yet, by not increasing the expression of endothelin, IGF-1 may control proliferation by preventing the formation of an autocrine positive-feedback loop. This suggestion needs to be more fully explored as IGF-1 might affect endothelin signaling via posttranscriptional and translational analysis methods.

IGF-1 also increased the expression of fatty-acid binding protein 3 (FABP3), otherwise known as mammary-derived growth inhibitor (MDGI). MDGI causes inhibition of cell proliferation in serum-deprived cells. MDGI inhibits MAC-T cell proliferation in a dose-dependent manner (Zavizion et al., 1993). However, this inhibition of growth disappears after six days of MDGI treatment. Furthermore, cell quiescence is required for the actions of MDGI as cells that were not serum-starved for 14 hours showed a minimal inhibition of proliferation (Zavizion et al., 1995). In our cell model, IGF-1 increased the expression of MDGI by almost 2-fold. One explanation for this seeming incongruous result is that cell-contact inhibition may be responsible for this increase. MAC-T cells proliferate in colonies (Huynh et al., 1991); consequently after a period of proliferation, cells will form large groups of cells. Cells along the fringe of the colony have room to divide; thus, they are not affected by cell crowding. However, they surround the cells in the center of the colony, which do not divide due to cell-contact inhibition. Related to this is evidence shows that MDGI transcripts are highly expressed in lactating mammary glands (Kurtz et al., 1990). Given that cell contact is a necessary condition for differentiation in cultured mammary cell models, the cells within each colony could be expressing MDGI to prepare the cells for differentiation. In mouse mammary explants treated with MDGI, lobuloalveolar formation and beta-casein expression was increased and epithelial cell growth was decreased (Kurtz et al., 1998). However, this needs to be explored further by estimating gene expression differences between crowded and not crowded cells.

Another reason that IGF-1 may increase the expression of MDGI is that the MDGI protein is a mixture of two fatty acid binding proteins with highly homologous sequences. Specht et al. (1996) demonstrated that the amino-acid sequence of heart-derived fatty acid binding protein (H-FABP, which is considered to be the MDGI protein) contains only 7 different amino acids compared with adipocyte-derived fatty acid binding protein. Furthermore, they discovered that MDGI mRNA from lactating bovine mammary tissue demonstrated the presence of the adipocyte-derived fatty acid binding protein along (A-FABP) with H-FABP. Whether A-FABP is the protein that inhibits proliferation has yet to be determined. However, Specht et al (1996) showed that H-FABP inhibited mammary cell proliferation. Therefore, the increase in MDGI mRNA in this experiment could be due to the presence of A-FABP mRNA.

Discussion of Approach

This experiment tested my hypothesis that IGF-1 alters the expression of genes in a manner consistent with increased proliferation in bovine mammary epithelial cells. The biological model used for this experiment was the MAC-T cell line, a transformed cell line. Transformation induces the cell to be able to continuously proliferate under the appropriate signal. Thus, one of the factors for continual proliferation could be a constant upregulation of proliferation-inducing genes or a constant downregulation of proapoptotic genes. An alternative model that could have been used is primary mammary epithelial cells. Primary cells are not transformed to continually proliferate, thereby avoiding a possible bias towards cell proliferation. However, primary cells can undergo senescence, in which they stop proliferating after being passaged too many times (Matitashvili et al, 1997). To test my hypothesis, it is critical that the cells proliferate in response to IGF-1. As previously discussed, MAC-T cells respond to IGF-1 by increasing proliferation. In fact, in my preliminary results, MAC-T cells treated with 100 ng/mL IGF-1 synthesized DNA at greater than 3 times the rate of control cells. Therefore, much of the signaling pathways are likely still intact in the MAC-T cells. While my study provides a foundation for understanding the effects of IGF-1 on gene expression in bovine mammary epithelial cells, future studies should be conducted to determine if primary mammary epithelial cells respond in a similar manner.

One effect that should be examined is the effect of substratum on gene expression. The MAC-T cells in this experiment were grown in collagen-coated flasks. However, a different substratum, such as a collagen gel, could alter gene expression in place of IGF-1. Huynh et al. (1991) showed that MAC-T cells grown on floating collagen gels produced more β-casein mRNA than cells plated on plastic substratum. When examining the differences between the clonal and parental MAC-T cells, Zavizion et al. (1995) noticed that one of the colonies grew in an atypical manner on collagen than the other colonies and the parental cell line. However, when treated with mammary extracts from prepubertal dairy heifers, cells plated on plastic substratum grew in a similar dose-dependent manner as cells plated on a collagen substratum (Berry et al. 2003).

To verify the biological actions of IGF-1 in this study, I measured cell confluency in the culture flasks. I wanted to confirm that the IGF-1 used in this genomics study was biologically active and was likely stimulating proliferation as it had in my preliminary study. Percentages of confluency were used to qualitatively verify the biological activity of IGF-1 without compromising my ability to isolate high-quality RNA from the cells. Previous studies have consistently shown that IGF-1 increases proliferation in MAC-T cells (Zhao et al., 1992; Woodward et al., 1994; Robinson et al., 2000). Furthermore, 100 ng/mL IGF-1 increased cell proliferation along with confluency in my preliminary study. Therefore, I was confident that because IGF-1 increased confluency in this genomics study, it likely also increased proliferation. However, I recognize that confluency is not necessarily proportional to rate of proliferation because confluency can be affected by changes in cell size.

In my project, I tried to collect mRNA at both 8 and 24 hr of control and IGF-1 treatments for each of three experiments. However, I did not collect quality mRNA from each sample of each experiment. Thus, I actually conducted four experiments instead of three. In experiment 1, all of the 24-hr mRNA was lost due to poor hybridizations, so gene expression from only the 8-hr arrays was measured. Experiment 2 worked as planned. The mRNA from the 24-hr cells was of high quality for both experiments 3 and 4. However, the mRNA from the control cells at 8 hr from experiment 3 and the mRNA from the IGF-1 treated cells at 8 hr from experiment 4 were degraded. Therefore, I used the mRNA from the 100 ng/ml treatment from experiment 3 and the mRNA from the 0 ng/ml treatment from experiment 4 as a set of 8-hr mRNA for treatment comparisons. I justify this because the MAC-T cells used in all of the experiments are from the same passage. Therefore, there should be very little genetic variation between the experiments, as confirmed by Table 5.

Even though the microarray analysis demonstrated changes in gene expression, these results were not confirmed for 4 of the 10 genes with qRT-PCR. One possible explanation is the number of biological replicates used in this experiment was too low to reduce the random variation. Three replicates of different culture times were used. A power test was not conducted because no previous data with the BMET array and the MAC-T cells were available. Three biological replicates were used to establish a foundation for determining the effects of IGF-1 on gene expression. However, this may not have been enough to detect significant changes in gene expression as measured with qRT-PCR.

The small sample number can affect the false discovery rate (FDR). The FDR is a statistic that calculates the probability of false discoveries that researchers are expecting to see in microarray data. Given that we had only three biological replicates, we would expect the FDR to be less significant. Pawitan et al. (2005) stated that to control for FDR the sample size should be large, for example, 45 arrays per group to get a 10% FDR if the proportion of non-significantly expressed genes is 99% and the researchers was to select the top 1% of significantly expressed genes. For smaller sets of arrays, genes must be highly significant to control for FDR. Given that we used a small set of arrays (6 arrays per time period), we would expect the FDR to be less significant.

Another effect that may explain the lack of significant results by qRT-PCR is the use of SYBR Green. SYBR Green is relatively inexpensive and easy to use. However, SYBR Green binds to any double-stranded nucleic acid sequence. Therefore, if primer dimers have formed between the forward and reverse primers for a gene of interest, the SYBR Green will incorrectly label that cDNA amplification product. Another RT-PCR procedure, the Taqman method, uses fluorescence tagged probes that bind to the target strand between where the two probes anneal. The ends of the probe are labeled with fluor tag and a quencher tag. Because the two tags are in close proximity, the quencher blocks light emission from the fluor. During RT-PCR, 5'-exonuclease of the Taq polymerase removes bases from the probe, including the fluor- and quencher-tagged bases. When these tagged bases are removed, the fluor emits light since it is not in as close proximity to the quencher. However, the fluor-tagged base only is cleaved when the probe anneals to it complementary sequence on the target gene transcript. Therefore, Taqman increases the sensitivity of RT-PCR.

Conclusion

The act of proliferation requires different cellular machinery than the act of differentiation. My hypothesis was that IGF-1 alters the expression of genes in a manner consistent with increased proliferation in bovine mammary epithelial cells. My objective was to determine if IGF-1 treatment for 8 and 24 hours alters the expression of genes in the MAC-T bovine mammary epithelial cell line in a manner consistent with increased proliferation.

In summary, IGF-1 increased cell confluency by 40% after 24 hr of treatment ($P < 0.05$). IGF-1 altered the expression ($P < 0.05$) of 89 genes after 8 hours (70 increased, 18 decreased) and 184 genes after 24 hours (139 increased, 45 decreased). IGF-1 altered the expression of several regulatory genes that might increase cell proliferation, such as those for polyamine synthesis, cell cycle progression, and stress response, and several other genes that support increased proliferation, such as metabolism and cell structure genes. The fold-changes of 9 of 10 genes as measured with RT-PCR were similar to those with microarray analysis, although the statistical significance of the change was the same for only 6 of the genes. In conclusion, IGF-1 alters the expression of proliferative and metabolic genes in a manner consistent with increased cell proliferation.

Transcriptional regulation is not the only mechanism that IGF-1 can use to promote proliferation. Proteins can be modified or destroyed, pathways can be sped up or slowed down, and physical migration of the cells may be increased or decreased. These mechanisms have been studied in other cell systems in other animals. Examining whether the same mechanisms are altered by IGF-1 in its mitogenic effects would assist in better understanding the biological effects of IGF-1 in the bovine mammary gland.

Appendix A

Introduction

This work was a preliminary project that I did before examining IGF-1 effects on gene expression. I include these results as an extension of my graduate work and not as part of the main thesis.

Leptin is a 16-kDa peptide that is secreted primarily by adipocytes and informs the brain on the energy status of the body. Feed intake increases circulating leptin levels in the body (Ahima and Flier, 2000). However, leptin has numerous other functions, including regulating cell proliferation (Maor et al., 2002). Circulating leptin levels are increased in dairy heifers fed to gain 1 or more kg/d (Block et al., 2003). Silva et al. (2002) hypothesized that leptin negatively affected the stimulatory actions of insulin-like growth factor 1 (IGF-1) on mammary epithelial cell proliferation in prepubertal Holstein heifers. To accomplish this, they infused four treatments, 0 or 100 μg leptin mixed with 0 or 10 μg IGF-1, into each of the four quarters of the mammary gland in six Holstein heifers. Based upon previous work, Silva (2002) showed that each quarter of a bovine mammary gland was not influenced by hormonal treatments in the other quarters and could act as its own experimental unit. The heifers were infused with the treatments once a day for 6 days then twice on day 7, with 14 hours separating the last two infusions. On day 8, the heifers were infused with bromodeoxyuridine (BrdU) for 2 hours, slaughtered, and the glands were sampled to measure incorporation of BrdU into the DNA of dividing cells. Silva found that quarters treated with leptin and IGF-1 showed reduced mammary development by 52% when compared to quarters treated IGF-1 alone.

While the results seem to implicate leptin as a mediator for decreased mammary development in heavy prepubertal heifers, the dose of leptin used could have been supraphysiological. Indeed, mammary extracts from leptin-treated quarters contained 171 ng leptin per mL extract, while saline treated quarters only contained around 4 ng/mL. Therefore, we hypothesized that smaller doses of leptin would also impair IGF-1-induced mammary epithelial cell growth, albeit at lower levels. My objective was to examine differences in mammary epithelial cell growth in quarters treated with three different doses of leptin. IGF-1 was included in all of the doses.

Materials and Methods

Two Holstein heifers (8 months, average 400 lbs) were obtained from and housed on the Michigan State University Dairy Cattle Teaching and Research Center. Using Spartan Dairy v 2.0, diets were designed for an average daily gain of 0.7 kg/d and a crude protein to metabolizable energy (CP/ME) ratio of approximately 60 g CP/Mcal ME. Throughout the adaptation and experimental periods, the heifers were housed in the metabolism unit and were exercised in a small paddock for about an hour per day. The heifers underwent a 19-day adaptation period in which they were accustomed to the diet and handling. Five days before the infusion period, the front quarters of each of the heifers was infused with 12 mL physiological saline. The infusions were administered using a 12 mL syringe and a modified 200-µL pipette tip in which part of the wide end was cut off for better attachment to the syringe. Each tip was covered in Surgilube to allow easier insertion of the tip into the teat. The heifers received the infusions at 0800 hours (hr) and their udders were palpated for mastitis at 1400 hr and 1700 hr. No hardness or soreness of the udder was detected. This project was approved by the Michigan State University All-University Committee on Animal Use and Care.

Lyophilized recombinant human IGF-1 (GroPep Pty, Adelaide) was reconstituted to 1 mg/mL in equal amounts of sterile 100 m*M* hydrochloric acid and sterile 100 m*M* sodium hydroxide and stored at -20°C. Recombinant ovine leptin was kindly provided by Dr. Ari Gertler, was reconstituted to 1 mg/mL in sterile MilliQ water and stored at -20°C. All infusions were prepared at 0600 and the animals were infused at 0800. The different doses of leptin (0, 23, 46 μg) were combined in 10 mL sterile physiological saline per treatment that also contained 1 μg/mL IGF-1 and 1 mg/mL bovine serum albumin. Each treatment was separated into 12-mL syringes and 200-μL pipette tips that were modified as described above and covered in Surgilube. The animals were allowed to exercise in a grassy paddock for one hour before infusions. Upon infusion, the teats were cleaned with 3% iodine and 70% ethanol. The hormones were infused in each animal according to the design shown in Figure 7.

Figure 7. Infusion design for the udder quarters of each heifer. Each quarter received 1 μg/mL IGF-1 and 1 mg/mL BSA along with the treatments daily for 7 days.

	4160		Front	4162		
Left	0 μg leptin	23 μg leptin		0 μg leptin	46 μg leptin	Right
	0 μg leptin	46 μg leptin		0 μg leptin	23 μg leptin	
			Rear			

Blood samples from either the tail vein or the jugular vein were obtained before the first infusion. On day 7, the heifers were infused at 0800 hr and again at 2000 hr.

On the day of slaughter, the animals were weighed and two blood samples were taken from the jugular vein of each heifer. BrdU (reconstituted to 10 mg/mL and pH set to 7.38, Sigma) was infused at an amount of 5 mg/kg BW via jugular catheter. Heifers were slaughtered between 2.5 to 2.75 hours later with 85 mg/kg body weight of sodium pentobarbital. The mammary gland was incised from each heifer and the sebaceous fluid was collected from the milk cistern of each quarter. 3 to 4 grams of parenchyma from each quarter was flash-frozen in liquid nitrogen. Parenchyma samples were taken from three regions in each quarter: the area proximal to the teat, the area opposite of the teat and closest to the fat pad and the area in between (labeled proximal, distal, and intermediate, respectively). Each sample was fixed in 10% formalin and shipped to the Diagnostic Center for Population and Animal Health for embedding. The University Animal Laboratory Resources disposed of the carcasses.

The immunohistochemistry protocol was adapted from Silva et al. (2000) and used the Zymed Histostain-SP kit. Briefly, tissue was sectioned into 6-μm slices and transferred to a poly-L-lysine-coated slide (Sigma-Aldritch). The slides were baked for 30 min at 65°C and then either were stained immediately after or transferred to –20°C for storage. The tissues were subjected to 3 xylene washes at 3 min per wash and then a series of decreasing ethanol washes (100%, 90%, and 70%) at 3 min each wash. The tissues were washed in methanol containing 3% hydrogen peroxide for 10 min and then a series of three phosphate-buffered saline (PBS) washes for 2 min per wash. The tissues were then immersed in citrate buffer (10 m*M*; pH 6.0) that was heated to between 90 and 95°C in a vegetable steamer. The tissues were heated for 20 min and then were cooled to 45°C. After another three washes in PBS for 2 min each wash, the tissue sections were immersed in PBS plus 5% nonimmune goat serum for 30 min in a humid chamber. The BrdU antibody (Clone 9318, Roche Applied Science) was diluted 1:50 in water containing 0.1% bovine serum albumin and 150 μL was applied to each section. The slides were then incubated at 4°C overnight in a humid chamber. The next day, the slides were washed in PBS (3 x 2 min) and then covered with a biotinylated secondary antibody for 10 min in a humid chamber. After another series of PBS washes, the tissues were covered with a streptavidin-peroxidase conjugate and incubated at room temperature in a humid chamber for 20 min. The tissues were washed again in PBS and were then exposed to diaminobenzidine in a humid chamber for 5 min at room temperature. The tissues were then rinsed in deionized water and covered with hematoxylin for 20 seconds. After being washed in PBS for 30 seconds, the tissues were washed in deionized water and subjected to an ascending series of ethanol washes (70%, 90%, and 100%) for 3 min per wash. The slides were washed in xylenes for 5 min and were mounted using Histomount and a 24 x 60 mm cover glass (Corning). Approximately 8 pictures were taken from each slide at using a Leica DFC480 camera attached to a Leica DM1L microscope (set to 40X) and hooked up to a Hewlett-Packard Pavilion a510n computer.

All epithelial cells were counted directly from the microscope until approximately 100 BrdU-positive cells were counted. Only the cells in the distal parenchymal region of the quarters were counted because there is evidence that more proliferation occurs in this region. This preliminary data would determine whether this would be a viable project to pursue. A serious problem that occurred was that much of the tissue failed to attach to the slide. The result was that, when viewed under a microscope, portions of the tissue would come out of focus relative to other portions of the tissues. Furthermore, parts of or the entire baked sectioned tissue would fall off the slide during the staining procedure. Consequently, it was extremely difficult in determining individual epithelial cells for counting. This was a continual occurrence with these tissues. It is believed that the paraffin did not fully invade the tissue since attempts to attach bovine mammary parenchymal tissue prepared by another scientist and rat mammary carcinoma tissue prepared by another outside laboratory proved successful. Alterations of batches of wash reagents used, changing the antigen presentation method (previously, the tissues were heated for 5 min, cooled for 5 min, heated again for 5 min and cooled to 45°C in 10 mM citrate buffer in a 600 MW microwave), using a different batch of poly-L-lysine slides, cooling the tissues before sectioning, and altering the wash times all proved unsuccessful in improving attachment of the tissues to the slide. Lack of resources and the increasing scarcity of tissue prevented the reparrafinization of the tissues. Counts were analyzed using the GLM procedure in SAS (v8.0) using treatment and heifer as classes.

The least squared means and standard deviations are presented in Figure 8. There was no difference in the number of BrdU-labeled cells between treatments (P = 0.9121) or heifers (P = 0.2593). It should be noted that only two heifers were used in this study and that this was preliminary data to determine whether to continue with the study. Furthermore, the standard deviation for the 46-µg leptin treatment is very high. This most likely was due to the difficulty in obtaining cell counts from the tissue; however, no statistical analyses were made to determine this. There were no differences in BrdU labeling between the three regions that were sampled.

Figure 8: Mean index of BrdU-labeled mammary epithelial cells sampled from two heifers infused once daily with 0, 23, or 46 μg leptin over a seven-day period.

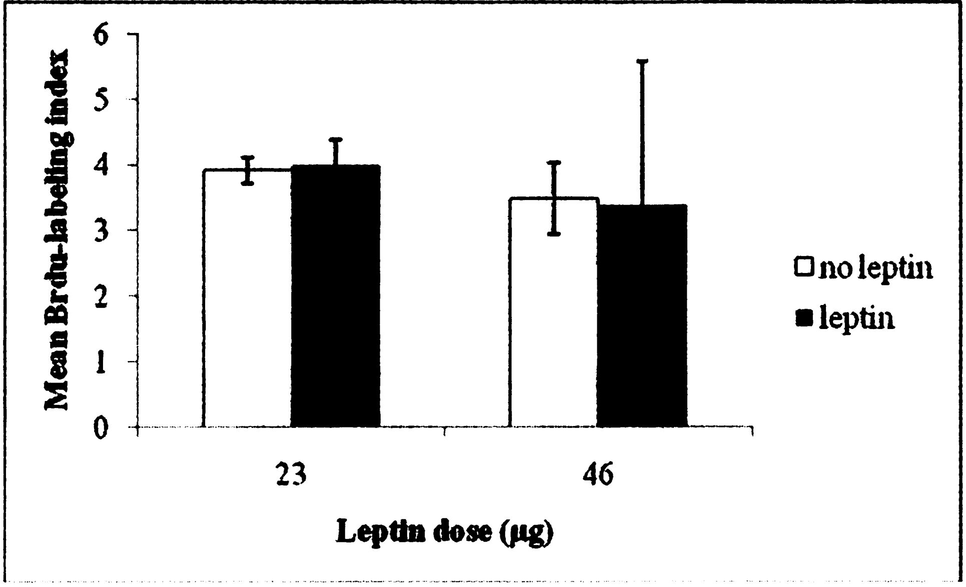

Appendix B

Upregulated in MAC-T cells after 24 hr of IGF-1 treatment.

Accession #	Gene Name	Fold-change	P-values	Symbol
Carbohydrate Metabolism				
CK965677	aldolase A, fructose-bisphosphate	1.29	0.05	ALDOA
CB433477	ATP citrate lyase	1.55	0.01	ACLY
AY508164.1	cadherin 1, type 1, E-cadherin (epithelial)	1.21	0.03	CDH1
CF613505	dihydrolipoamide S-acetyltransferase (E2 component of pyruvate dehydrogenase complex)	1.26	0.04	DLAT
CK949721	GDP-mannose pyrophosphorylase B	1.24	0.02	GMPPB
AF043228.1	glucose phosphate isomerase	1.55	0.04	GPI
NM_174319.1	hexokinase 1	1.22	0.03	HK1
CK952050	hexokinase 2	1.92	0.01	HK2
AF090321.1	isocitrate dehydrogenase 3 (NAD+) beta	1.22	0.01	IDH3B
NM_174099.2	lactate dehydrogenase A	1.39	<0.01	LDHA
NM_174100.1	lactate dehydrogenase B	1.22	0.01	LDHB
Bauman2461	lipase A, lysosomal acid, cholesterol esterase (Wolman disease)	1.26	0.03	LIPA
CK948244	malate dehydrogenase 1, NAD (soluble)	1.22	0.01	MDH1
CK772109	phosphogluconate dehydrogenase	1.33	0.03	PGD
CK849264	phosphoglycerate kinase 1	1.40	<0.01	PGK1
CK769449	phosphomannomutase 2	1.26	0.01	PMM2
CK775519	protease, serine, 16 (thymus)	1.21	0.01	PRSS16
CB165376	triosephosphate isomerase 1	1.40	0.02	TPI1
NM_174211.2	UDP-glucose dehydrogenase	1.22	<0.01	UGDH
Cell signaling				
AJ491865.1	5-hydroxytryptamine (serotonin) receptor 2C	1.44	0.01	HTR2C
AJ277986.1	angiotensin II receptor, type 2	1.22	0.01	AGTR2
NM_174308.1	endothelin receptor type A	1.47	0.01	EDNRA
NM_174556.1	insulin-like growth factor binding protein 3	1.42	0.01	IGFBP3
NM_174375.2	KIT ligand	1.31	0.01	KITLG
NM_174753.1	parathyroid hormone-like hormone	1.20	0.05	PTHLH
AW465454	stratifin	1.33	0.01	SFN
CK948130	transferrin receptor (p90, CD71)	1.32	0.04	TFRC
Cell Cycle and Death				

NM_174003.2	calpastatin	1.31	<0.01	CAST
CK960396	CDC6 cell division cycle 6 homolog (S. cerevisiae)	1.58	0.02	CDC6
CK846204	chromatin assembly factor 1, subunit A (p150)	1.22	0.01	CHAF1A
BM287438	cyclin E1	1.31	0.04	CCNE1
CB438089	tumor necrosis factor (ligand) superfamily, member 10	1.33	0.01	TNFSF10
Cell Structure and Extracellular Matrix				
CK769227	abl interactor 2	1.23	0.02	ABI2
CB222344	formin-like 2	1.24	<0.01	FMNL2
NM_173934.1	lumican	1.31	0.01	LUM
NM_174764.2	neural precursor cell expressed, developmentally down-regulated 8	1.23	<0.01	NEDD8
NM_174718.1	pinin, desmosome associated protein	1.61	0.01	PNN
Coagulation Factors				
J00007.1	coagulation factor IX (plasma thromboplastic component, Christmas disease, hemophilia B)	1.25	0.04	F9
CK777838	coagulation factor XIII, A1 polypeptide	1.27	0.01	F13A1
NM_174137.2	serine (or cysteine) proteinase inhibitor, clade E (nexin, plasminogen activator inhibitor type 1), member 1	1.53	0.02	SERPINE1
CK776402	tissue factor pathway inhibitor (lipoprotein-associated coagulation inhibitor)	1.25	<0.01	TFPI
DNA Replication and Repair				
CK846301	polymerase (DNA directed), epsilon 2 (p59 subunit)	1.31	0.01	POLE2
CB426829	RAN, member RAS oncogene family	1.35	0.03	RAN
Energy Metabolism				
CK941391	aldehyde dehydrogenase 18 family, member A1	1.25	0.04	ALDH18A1
BF775817	coproporphyrinogen oxidase	1.41	<0.01	CPOX
CK964867	cytochrome P450, family 26, subfamily B, polypeptide 1	1.35	0.05	CYP26B1
NM_177502.2	glutamic-oxaloacetic transaminase 1, soluble (aspartate aminotransferase 1)	1.32	0.02	GOT1
CB453756	heme oxygenase (decycling) 2	1.45	<0.01	HMOX2
CK974609	holocytochrome c synthase	1.21	0.03	HCCS

	(cytochrome c heme-lyase)			
CK772343	hydroxymethylbilane synthase	1.29	0.04	HMBS
NM_175820.2	NADH dehydrogenase (ubiquinone) 1 alpha subcomplex, 4, 9kDa	1.27	0.02	NDUFA4
NM_175791.2	NADH dehydrogenase (ubiquinone) 1 alpha subcomplex, 6, 14kDa	1.21	0.01	NDUFA6
CB468421	NADH dehydrogenase (ubiquinone) 1, alpha/beta subcomplex, 1, 8kDa	1.22	0.02	NDUFAB1
NM_174564.2	NADH dehydrogenase (ubiquinone) 1, subcomplex unknown, 1, 6kDa	1.27	0.02	NDUFC1
NM_175800.2	NADH dehydrogenase (ubiquinone) Fe-S protein 4, 18kDa (NADH-coenzyme Q reductase)	1.23	<0.01	NDUFS4
NM_173968.2	thioredoxin	1.31	0.02	TXN
Folate Metabolism				
BP100358	gamma-glutamyl hydrolase (conjugase, folylpolygammaglutamyl hydrolase)	1.22	0.01	GGH
CK960935	methylenetetrahydrofolate dehydrogenase (NADP+ dependent), methenyltetrahydrofolate cyclohydrolase	1.41	0.01	MTHFD1
CK775888	sepiapterin reductase (7,8-dihydrobiopterin:NADP+ oxidoreductase)	1.38	0.02	SPR
Glycan Metabolism				
CK972901	asparagine-linked glycosylation 5 homolog (yeast, dolichyl-phosphate beta-glucosyltransferase)	1.21	0.04	ALG5
AW425955	asparagine-linked glycosylation 6 homolog (yeast, alpha-1,3-glucosyltransferase)	1.21	<0.01	ALG6
CK845990	core 1 UDP-galactose:N-acetylgalactosamine-alpha-R beta 1,3-galactosyltransferase	1.23	0.02	C1GALT1
NM_177498.2	farnesyltransferase, CAAX box, alpha	1.30	0.02	FNTA
NM_177501.1	fucosyltransferase 8 (alpha (1,6) fucosyltransferase)	1.24	0.03	FUT8
CK769632	glucosidase I	1.24	0.01	GCS1
AW426143	Rab geranylgeranyltransferase, beta subunit	1.27	0.02	RABGGTB
Lipid Metabolism				

CK973155	acetyl-Coenzyme A acyltransferase 2 (mitochondrial 3-oxoacyl-Coenzyme A thiolase)	1.22	0.01	ACAA2
CK846911	acyl-CoA synthetase long-chain family member 6	1.22	<0.01	ACSL6
CK778309	dual-specificity tyrosine-(Y)-phosphorylation regulated kinase 3	1.28	0.04	DYRK3
CB444358	elongation of very long chain fatty acids (FEN1/Elo2, SUR4/Elo3, yeast)-like 4	1.30	0.02	ELOVL4
NM_177497.2	farnesyl diphosphate synthase (farnesyl pyrophosphate synthetase, dimethylallyltranstransferase, geranyltranstransferase)	1.26	<0.01	FDPS
CK944276	glycerol kinase	1.28	0.01	GK
CK771258	lysophospholipase I	1.28	0.05	LYPLA1
CK776702	phosphatidylinositol glycan, class B	1.27	0.03	PIGB
Bauman781	phytoceramidase, alkaline	1.34	0.02	PHCA
CK832399	putative acyl-CoA dehydrogenase	1.24	0.05	FLJ12592
Protein Synthesis and Metabolism				
CK848612	aminolevulinate, delta-, synthase 1	1.22	<0.01	ALAS1
NM_175813.1	eukaryotic translation initiation factor 2, subunit 1 alpha, 35kDa	1.40	0.01	EIF2S1
CB534551	eukaryotic translation initiation factor 4A, isoform 1	1.31	0.02	EIF4A1
CB444175	glutamate-cysteine ligase, catalytic subunit	1.64	0.02	GCLC
CK948205	glutathione peroxidase 2 (gastrointestinal)	1.26	0.01	GPX2
CB171170	glutathione S-transferase omega 1	1.24	0.02	GSTO1
CK968451	glycyl-tRNA synthetase	1.23	0.01	GARS
AV602991	lysyl-tRNA synthetase	1.20	0.04	KARS
CB451602	mitochondrial ribosomal protein S14	1.22	0.01	MRPS14
NM_174130.2	ornithine decarboxylase 1	1.47	0.01	ODC1
CK953114	phenylalanine-tRNA synthetase-like, beta subunit	1.25	0.05	FARSLB
CB458343	serine hydroxymethyltransferase 2 (mitochondrial)	1.30	<0.01	SHMT2
NM_174175.2	seryl-tRNA synthetase	1.29	<0.01	SARS
BI898927	spermidine synthase	1.36	0.02	SRM
Purine and Pyrimidine Metabolism				
CK983189	adenosine kinase	1.22	0.01	ADK
NM_173889.1	adenylate kinase 2	1.42	0.01	AK2
CK772896	dihydroorotate dehydrogenase	1.53	<0.01	DHODH

CB172231	IMP (inosine monophosphate) dehydrogenase 2	1.33	0.05	IMPDH2
CK849436	nucleoside phosphorylase	1.34	<0.01	NP
CK777978	phosphoribosyl pyrophosphate synthetase 1	1.23	0.01	PRPS1
CK958159	phosphoribosylglycinamide formyltransferase, phosphoribosylglycinamide synthetase, phosphoribosylaminoimidazole synthetase	1.36	0.01	GART
CK979761	ribonucleotide reductase M2 polypeptide	1.71	0.01	RRM2
NM_174625.2	thioredoxin reductase 1	1.47	<0.01	TXNRD1
CK970228	UMP-CMP kinase	1.24	0.01	UMP-CMPK
NM_177508.1	uridine monophosphate synthetase (orotate phosphoribosyl transferase and orotidine-5'-decarboxylase)	1.39	0.02	UMPS
Signal Transduction				
CL513Contig1	chemokine (C-C motif) ligand 4-like	1.25	0.01	CCL4L
CK846020	FOS-like antigen 1	1.41	0.01	FOSL1
BF606842	heat shock 70kDa protein 5 (glucose-regulated protein, 78kDa)	1.33	<0.01	HSPA5
AB072368.1	heat shock 90kDa protein 1, alpha	1.36	0.03	HSPCA
BI538908	mitogen-activated protein kinase 6	1.29	0.02	MAPK6
CK838207	mitogen-activated protein kinase kinase kinase 7 interacting protein 2	1.22	0.05	MAP3K7IP2
CK777104	mitogen-activated protein kinase-activated protein kinase 3	1.25	0.03	MAPKAPK3
BP106653	nuclear factor of activated T-cells, cytoplasmic, calcineurin-dependent 3	1.29	0.04	NFATC3
BM431413	pleiotropic regulator 1 (PRL1homolog, Arabidopsis)	1.33	<0.01	PLRG1
NM_174586.1	protein kinase, AMP-activated, gamma 1 non-catalytic subunit	1.23	0.04	PRKAG1
NM_181031.2	protein phosphatase 2 (formerly 2A), catalytic subunit, alpha isoform	1.21	0.04	PPP2CA
CK770419	RuvB-like 1 (E. coli)	1.32	0.01	RUVBL1
BM364201	suppressor of cytokine signaling 1	1.26	0.05	SOCS1
BM435193	TGFB inducible early growth response	1.39	0.01	TIEG
CK953368	tyrosine 3-monooxygenase/tryptophan 5-	1.28	0.01	YWHAQ

	monooxygenase activation protein, theta polypeptide			
Transcription				
CK728106	activated RNA polymerase II transcription cofactor 4	1.30	0.04	PC4
CL3817Contig1	ets variant gene 1	1.39	0.02	ETV1
CK971624	general transcription factor IIB	1.23	<0.01	GTF2B
CB461430	methyl-CpG binding domain protein 2	1.30	0.02	MBD2
CK951297	pleiomorphic adenoma gene-like 2	1.21	0.01	PLAGL2
AF461104.1	polymerase (RNA) I polypeptide B, 128kDa	1.26	0.04	POLR1B
CK838008	suppressor of S. cerevisiae gcr2	1.30	0.04	HSGT1
CK955167	T-box 3 (ulnar mammary syndrome)	1.47	0.03	TBX3
CK774454	transcription elongation factor B (SIII), polypeptide 3 (110kDa, elongin A)	1.21	0.02	TCEB3
CK769868	transcription factor-like 4	1.29	0.03	TCFL4
BF605641	zinc ribbon domain containing, 1	1.40	0.01	ZNRD1
Transport				
CB462017	ATP-binding cassette, sub-family A (ABC1), member 1	1.24	0.01	ABCA1
AB006985.1	ATP-binding cassette, sub-family B (MDR/TAP), member 1	1.37	<0.01	ABCB1
NM_174313.2	fatty acid binding protein 3, muscle and heart (mammary-derived growth inhibitor)	1.95	<0.01	FABP3
NM_174602.2	solute carrier family 2 (facilitated glucose transporter), member 1	1.21	<0.01	SLC2A1
NM_174658.1	solute carrier family 25 (mitochondrial carrier; adenine nucleotide translocator), member 4	1.29	0.01	SLC25A4
CB165860	solute carrier family 3 (activators of dibasic and neutral amino acid transport), member 2	1.33	0.02	SLC3A2
Unknown				
CB533649	factor for adipocyte differentiation 158	1.22	0.01	FAD158
CK848911	FK506 binding protein 1A, 12kDa	1.22	0.03	FKBP1A
CB430950	hypothetical protein MGC2744	1.21	<0.01	MGC2744
CK946480	RAB27A, member RAS oncogene family	1.22	0.04	RAB27A
CB535077	SH3-domain kinase binding protein 1	1.30	0.02	SH3KBP1

AF198054.1	1.70	<0.01
NM_181810.1	1.28	<0.01
NM_174662.2	1.32	0.02

Appendix C

Downregulated genes in MAC-T cells after 24 hr of IGF-1 treatment.

Accession #	Gene Name	Fold change	P-value	Symbol
Carbohydrate Metabolism				
CB454232	mannosidase, alpha, class 2A, member 1	0.67	<0.01	MAN2A1
CK770297	UDP-Gal:betaGlcNAc beta 1,4-galactosyltransferase, polypeptide 5	0.78	0.04	B4GALT5
NM_174224.2	acetyl-Coenzyme A carboxylase alpha	0.79	0.02	ACACA
Cell Cycle and Death				
CK944043	cyclin-dependent kinase inhibitor 2B (p15, inhibits CDK4)	0.77	0.01	CDKN2B
CL8903Contig1	A kinase (PRKA) anchor protein 8	0.78	0.02	AKAP8
Cell signaling				
AY486452.1	epidermal growth factor receptor (erythroblastic leukemia viral (v-erb-b) oncogene homolog, avian)	0.75	<0.01	EGFR
NM_181010.2	endothelin 1	0.66	<0.01	EDN1
NM_194266.1	adrenergic, beta-1-, receptor	0.78	0.01	ADRB1
NM_174555.1	insulin-like growth factor binding protein 2, 36kDa	0.78	0.02	IGFBP2
Cell Structure and Extracellular Matrix				
CK941880	lamin B2	0.78	0.02	LMNB2
CK944548	nuclear mitotic apparatus protein 1	0.78	0.02	NUMA1
CB468342	dedicator of cytokinesis 1	0.68	0.01	DOCK1
AB055312.1	cathepsin D (lysosomal aspartyl protease)	0.76	0.01	CTSD
CK776003	collagen, type IV, alpha 6	0.74	0.04	COL4A6
BE752701	agrin	0.79	0.03	AGRN
CK975649	gelsolin (amyloidosis, Finnish type)	0.70	0.02	GSN
DNA Replication and Repair				
CB420483	MAX interactor 1	0.67	0.01	MXI1
Energy Metabolism				
NM_174304.1	cytochrome P450, family 17, subfamily A, polypeptide 1	0.80	0.05	CYP17A1
Lipid Metabolism				
CK948274	aldehyde dehydrogenase 3 family, member A2	0.78	0.03	ALDH3A2
CK971583	sialyltransferase 7 ((alpha-N-acetylneuraminyl-2,3-beta-galactosyl-1,3)-N-acetyl galactosaminide alpha-2,6-	0.75	0.01	SIAT7B

	sialyltransferase) B			
NM_177521.2	sulfotransferase family, cytosolic, 1A, phenol-preferring, member 1	0.67	0.04	SULT1A1
CK774100	peroxisomal long-chain acyl-coA thioesterase	0.74	0.04	ZAP128
Protein Synthesis and Metabolism				
CK849902	methionine adenosyltransferase II, beta	0.79	0.01	MAT2B
CK833665	alanyl (membrane) aminopeptidase (aminopeptidase N, aminopeptidase M, microsomal aminopeptidase, CD13, p150)	0.79	0.02	ANPEP
AW658968	histidine decarboxylase	0.55	<0.01	HDC
Purine and Pyrimidine Metabolism				
CK769403	adenylate cyclase 8 (brain)	0.72	0.01	ADCY8
Signal Transduction				
CK945745	mitogen-activated protein kinase 4	0.74	<0.01	MAPK4
CK950713	inhibitor of DNA binding 1, dominant negative helix-loop-helix protein	0.67	0.03	ID1
CK770014	inhibitor of DNA binding 3, dominant negative helix-loop-helix protein	0.73	0.01	ID3
CK943734	frizzled homolog 4 (Drosophila)	0.72	0.02	FZD4
CB467921	beta-transducin repeat containing	0.76	0.04	BTRC
CB422127	nuclear factor of activated T-cells 5, tonicity-responsive	0.77	0.03	NFAT5
CK777672	retinoic acid receptor, beta	0.63	0.02	RARB
AV610239	insulin receptor substrate 1	0.76	0.01	IRS1
CK778883	ral guanine nucleotide dissociation stimulator	0.74	<0.01	RALGDS
Transcription				
CK974450	basic transcription factor 3	0.77	0.03	BTF3
AV591750	zinc finger protein 192	0.77	<0.01	ZNF192
CB531176	general transcription factor II, i	0.80	<0.01	GTF2I
BM481287	homeo box D10	0.43	0.03	HOXD10
CL1270Contig1	cellular repressor of E1A-stimulated genes 1	0.65	0.02	CREG1
AY398689.1	microphthalmia-associated transcription factor	0.71	0.03	MITF
CK972308	UBX domain containing 2	0.78	<0.01	UBXD2
CK837990	ets variant gene 1	0.76	0.01	ETV1
Transport				
BE217451	solute carrier family 39 (zinc transporter), member 6	0.74	<0.01	SLC39A6

CB442833	solute carrier family 1 (glial high affinity glutamate transporter), member 2	0.78	<0.01	SLC1A2

Appendix D

Upregulated genes in MAC-T cells after 8 hr of IGF-1 treatment.

Accession #	Gene Name	Fold-change	P-value	Symbol
Carbohydrate Metabolism				
AF054834.1	amylase, alpha 2B; pancreatic	1.25	0.03	AMY2B
CB433477	ATP citrate lyase	1.33	0.03	ACLY
AF461103.1	citrate synthase	1.28	<0.01	CS
NM_174319.1	hexokinase 1	1.26	0.02	HK1
NM_174100.1	lactate dehydrogenase B	1.24	<0.01	LDHB
CK770445	malic enzyme 1, NADP(+)-dependent, cytosolic	1.44	0.01	ME1
CK849264	phosphoglycerate kinase 1	1.22	<0.01	PGK1
CK769449	phosphomannomutase 2	1.44	0.05	PMM2
NM_175814.2	succinate dehydrogenase complex, subunit C, integral membrane protein, 15kDa	1.23	0.03	SDHC
DNA Replication and Repair				
CK846204	chromatin assembly factor 1, subunit A (p150)	1.28	0.05	CHAF1A
NM_182651.1	DNA (cytosine-5-)-methyltransferase 1	1.30	0.01	DNMT1
CK960935	methylenetetrahydrofolate dehydrogenase (NADP+ dependent), methenyltetrahydrofolate cyclohydrolase, formyltetrahydrofolate synthetase	1.52	0.01	MTHFD1
CK940683	replication protein A1, 70kDa	1.22	0.02	RPA1
Cell signaling				
AJ491865.1	5-hydroxytryptamine (serotonin) receptor 2C	1.28	0.01	HTR2C
AY191360.2	epidermal growth factor (beta-urogastrone)	1.44	<0.01	EGF
NM_174556.1	insulin-like growth factor binding protein 3	1.40	0.03	IGFBP3
AW465454	stratifin	1.35	0.03	SFN
Signal Transduction				
CK846020	FOS-like antigen 1	1.38	0.04	FOSL1
NM_174586.1	protein kinase, AMP-activated, gamma 1 non-catalytic subunit	1.34	0.02	PRKAG1
Bauman1784	protein kinase, cGMP-dependent, type II	1.30	0.03	PRKG2
CK773728	protein tyrosine phosphatase, receptor type, R	1.38	0.01	PTPRR

Energy Metabolism				
CK964867	cytochrome P450, family 26, subfamily B, polypeptide 1	1.70	0.02	CYP26B1
CK974609	holocytochrome c synthase (cytochrome c heme-lyase)	1.29	0.02	HCCS
CK772343	hydroxymethylbilane synthase	1.35	0.04	HMBS
NM_175809.1	NADH dehydrogenase (ubiquinone) 1 beta subcomplex, 1, 7kDa	1.22	0.05	NDUFB1
NM_174564.2	NADH dehydrogenase (ubiquinone) 1, subcomplex unknown, 1, 6kDa	1.23	0.03	NDUFC1
Cell Cycle and Death				
CK960396	CDC6 cell division cycle 6 homolog (S. cerevisiae)	1.85	0.03	CDC6
BM287438	cyclin E1	1.37	0.03	CCNE1
Lipid Metabolism				
NM_177497.2	farnesyl diphosphate synthase (farnesyl pyrophosphate synthetase, dimethylallyltranstransferase, geranyltranstransferase)	1.42	<0.01	FDPS
BM251520	insulin induced gene 1	1.21	0.02	INSIG1
Protein Synthesis and Metabolism				
CK773538	acetyl-Coenzyme A acetyltransferase 2 (acetoacetyl Coenzyme A thiolase)	1.32	0.03	ACAT2
CB534551	eukaryotic translation initiation factor 4A, isoform 1	1.54	0.02	EIF4A1
NM_177515.2	glutathione S-transferase A1	1.25	0.04	GSTA1
CK848917	histidyl-tRNA synthetase	1.23	0.02	HARS
CK976501	hypothetical protein FLJ22649 similar to signal peptidase SPC22/23	1.23	0.01	FLJ22649
NM_174130.2	ornithine decarboxylase 1	1.60	<0.01	ODC1
CK771294	phosphoglycerate dehydrogenase	1.37	0.03	PHGDH
CB168605	ribophorin I	1.24	0.01	RPN1
BM258870	serine dehydratase	1.35	0.05	SDS
CK951402	vanin 1	1.29	<0.01	VNN1
Purine and Pyrimidine Metabolism				
CK769403	adenylate cyclase 8 (brain)	1.24	0.01	ADCY8
NM_173889.1	adenylate kinase 2	1.51	0.02	AK2
CK849570	adenylosuccinate lyase	1.30	0.04	ADSL
CK772896	dihydroorotate dehydrogenase	1.52	0.05	DHODH
CB172231	IMP (inosine monophosphate) dehydrogenase 2	1.70	0.02	IMPDH2
CK777978	phosphoribosyl pyrophosphate synthetase 1	1.38	0.02	PRPS1
CK979761	ribonucleotide reductase M2 polypeptide	1.62	0.02	RRM2

NM_177508.1	uridine monophosphate synthetase (orotate phosphoribosyl transferase and orotidine-5'-decarboxylase)	1.69	0.01	UMPS
Cell Structure and Extracellular Matrix				
NM_174307.2	dermatan sulfate proteoglycan 3	1.29	0.03	DSPG3
AW356495	transient receptor potential cation channel, subfamily C, member 6	1.32	0.01	TRPC6
Transcription				
CB420822	basic helix-loop-helix domain containing, class B, 2	1.22	0.03	BHLHB2
NM_174000.2	calreticulin	1.26	0.01	CALR
CB531724	LAG1 longevity assurance homolog 2 (S. cerevisiae)	1.22	<0.01	LASS2
CK778210	nuclear receptor subfamily 4, group A, member 3	1.47	0.01	NR4A3
AF461104.1	polymerase (RNA) I polypeptide B, 128kDa	1.33	0.05	POLR1B
CK770419	RuvB-like 1 (E. coli)	1.48	0.04	RUVBL1
CK847247	SWI/SNF related, matrix associated, actin dependent regulator of chromatin, subfamily a, member 4	1.20	0.02	SMARCA4
CK976188	TAF12 RNA polymerase II, TATA box binding protein (TBP)-associated factor, 20kDa	1.31	0.02	TAF12
CK980388	TAF2 RNA polymerase II, TATA box binding protein (TBP)-associated factor, 150kDa	1.24	0.01	TAF2
CK955167	T-box 3 (ulnar mammary syndrome)	1.28	0.03	TBX3
CK774454	transcription elongation factor B (SIII), polypeptide 3 (110kDa, elongin A)	1.26	0.04	TCEB3
Transport				
CB462017	ATP-binding cassette, sub-family A (ABC1), member 1	1.28	0.04	ABCA1
NM_174313.2	fatty acid binding protein 3, muscle and heart (mammary-derived growth inhibitor)	2.13	<0.01	FABP3
CK848911	FK506 binding protein 1A, 12kDa	1.22	0.04	FKBP1A
BM030917	solute carrier family 25 (mitochondrial carrier; ornithine transporter) member 15	1.20	<0.01	SLC25A15
NM_174657.2	solute carrier family 25 (mitochondrial carrier; phosphate carrier), member 3	1.21	0.04	SLC25A3
CB165860	solute carrier family 3 (activators of dibasic and neutral amino acid transport), member 2	1.32	0.04	SLC3A2

Unknown				
CK943898	polyamine-modulated factor 1	1.54	0.02	PMF1
AF198054.1		1.28	0.01	
NM_174086.1		1.53	<0.01	

Appendix E

Downregulated genes after 8 hr of IGF-1 treatment.

Accession #	Gene Name	Fold-change	P-value	Symbol
Cell Structure and Extracellular Matrix				
BM258099	v-erb-b2 erythroblastic leukemia viral oncogene homolog 2, neuro/glioblastoma derived oncogene homolog (avian)	0.69	0.01	ERBB2
Energy Metabolism				
AY265991.1	cytochrome P450, family 1, subfamily A, polypeptide 2	0.79	0.01	CYP1A2
Lipid Metabolism				
CK971583	sialyltransferase 7 ((alpha-N-acetylneuraminyl-2,3-beta-galactosyl-1,3)-N-acetyl galactosaminide alpha-2,6-sialyltransferase) B	0.79	0.04	SIAT7B
AW653508	diacylglycerol kinase, alpha 80kDa	0.78	0.02	DGKA
Protein Synthesis and Metabolism				
NM_173939.1	methylmalonyl Coenzyme A mutase	0.77	0.02	MUT
CK959627	propionyl Coenzyme A carboxylase, alpha polypeptide	0.79	0.03	PCCA
CB453808	3'-phosphoadenosine 5'-phosphosulfate synthase 1	0.73	0.01	PAPSS1
CK772118	cysteine sulfinic acid decarboxylase	0.76	0.04	CSAD
NM_180995.2	dopamine beta-hydroxylase (dopamine beta-monooxygenase)	0.77	0.03	DBH
Transcription				
CK837990	ets variant gene 1	0.73	0.01	ETV1
CK957547	GRB2-associated binding protein 1	0.72	0.05	GAB1
CB468243	transcription factor 12 (HTF4, helix-loop-helix transcription factors 4)	0.71	0.05	TCF12
AV664749	zinc finger protein 42 (myeloid-specific retinoic acid-responsive)	0.68	0.01	ZNF42
CK778931	piggyBac transposable element derived 1	0.78	<0.01	PGBD1
Signal Transduction				
CK953091	protein inhibitor of activated STAT, 1	0.73	0.04	PIAS1
CB439479	protein kinase C, eta	0.78	0.01	PRKCH
CK943734	frizzled homolog 4 (Drosophila)	0.74	0.05	FZD4
CK847494	lymphoid enhancer-binding factor 1	0.77	0.03	LEF1
Unknown				
AB019395.1		0.80	0.04	

Bibliography

Adesanya OO, Zhou J, Samathanam C, Powell-Braxton L, Bondy CA. Insulin-like growth factor 1 is required for G2 progression in the estradiol-induced mitotic cycle. Proc Natl Acad Sci USA 96 (1999): 3287-3291.

Ahima RS, Flier JS. Leptin. Annu Rev Physiol 62 (2000): 413-437.

Akers, R. Michael. Lactation and the mammary gland. Ames, Iowa : Iowa State University Press, 2002.

Akers, RM. Major advances in hormone and growth factor regulation of mammary growth and lactation in dairy cows. J Dairy Sci 89 (2006): 1222-1234.

Baker J, Liu JP, Robertson EJ, Efstratiadis A. Role of insulin-like growth factors in embryonic and postnatal growth. Cell 75 (1993): 73-82.

Battistini B, Chailler P, D'Orleans-Juste P, Briere N, Sirois P. Growth regulatory properties of endothelins. Peptides 14 (1993): 385-399.

Baumrucker CR, Stemberger BH. Insulin and insulin-like growth factor-I stimulate DNA synthesis in bovine mammary tissue in vitro. J Anim Sci 67 (1989): 3503-3514.

Berry SD, McFadden TB, Pearson RE, Akers RM. A local increase in the mammary IGF-1: IGFBP-3 ratio mediates the mammogenic effects of estrogen and growth hormone. Domest Anim Endocrinol 21 (2001): 39-53.

Berry SD, Howard RD, Jobst PM, Jiang H, Akers RM. Interactions between the ovary and the local IGF-I axis modulate mammary development in prepubertal heifers. J Endocrinol 177 (2003a): 295-304.

Berry SD, Weber Nielsen MS, Sejrsen K, Pearson RE, Boyle PL, Akers RM. Use of an immortalized bovine mammary epithelial cell line (MAC-T) to measure the mitogenic activity of extracts from heifer mammary tissue: effects of nutrition and ovariectomy. Domest Anim Endocrinol 25 (2003b): 245-253.

Bionaz M, Loor JJ. Identification of reference genes for quantitative real-time PCR in the bovine mammary gland during the lactation cycle. Physiol Genomics 29 (2007): 312-319.

Blat C, Delbe J, Villaudy J, Chatelain G, Golde A, Harel L. Inhibitory diffusible factor 45 bifunctional activity. As a cell growth inhibitor and as an insulin-like growth factor I-binding protein. J Biol Chem 264 (1989): 12449-12454 .

Block SS, Smith JM, Ehrhardt RA, Diac MC, Rhoads RP, Van Amburgh ME, Boisclair YR. Nutritional and developmenta regulation of plasma leptin in dairy cattle. J Dairy Sci 86 (2003): 3206-3214.

Butler AA, Shoshana Y, Gewolb IH, Karas M, Okubo Y, LeRoith D. Insulin-like growth factor-1 receptor signal transduction: at the interface between physiology and cell biology. Comp Biochem Physiol B 121 (1998): 19-26.

Campbell PG, Skaar TC, Vega JR, Baumrucker CR. Secretion of insulin-like growth factor-I (IGF-I) and IGF-binding proteins from bovine mammary tissue in vitro. J Endocrinol 128 (1991): 219-228.

Caruso A, Pellati A, Bosi P, Arena N, Stabellini G. Effects of spermidine synthase inhibition in cultured chick embryo fibroblasts. Cell Biol Int Rep 16(1992): 349-358.

Cohick WS, Turner JD. Regulation of IGF binding protein synthesis by a bovine mammary epithelial cell line. J Endocrionl 157 (1998): 327-336.

Collier RJ, McGrath MF, Byatt JC & Zurfluh LL. Regulation of bovine mammary growth by peptide hormones: involvement of receptors, growth factors and binding proteins. Livestock Prod Sci 35 (1993): 21–33.

Conover CA, Kiefer MC. Regulation and biological effect of endogenous insulin-like growth factor binding protein-5 in human osteoblastic cells. J Clin Endocrinol Metab 76 (1993):1153-1159.

Daughaday WH, Reeder C. Synchronous activation of DNA synthesis in hypophysectomized rat cartilage by growth hormone. J Lab Clin Med 68 (1966): 357-68.

Daughaday WH, Hall K, Raben MS, Salmon WD Jr, van den Brande JL, van Wyk JJ. Somatomedin: proposed designation for sulphation factor. Nature 235 (1972): 107.

Davis-Rinker LED. 2005 Nutritional influences on body and mammary growth and effect of leptin and IGF-1 in prepubertal dairy heifers. Ph.D. Thesis. Michigan State University, East Lansing.

De Meyts P, Palsgaard J, Sajid W, Theede AM, Aladdin H. Structural biology of insulin and IGF-1 receptors. Novartis Found Symp 262 (2004): 160-71.

D'Ercole AJ, Applewhite GT, Underwood LE. Evidence that somatomedin is synthesized by multiple tissues in the fetus. Dev Biol 75 (1980): 315-28.

Denko CW, Bergenstal DM. The effect of hypophysectomy and growth hormone on S35 fixation in cartilage. Endocrinology 57 (1955): 76-86.

Dufourny B, Alblas J, van Teeffelen HA, van Schaik FM, van der Burg B, Steenbergh PH, Sussenbach JS. Mitogenic signaling of insulin-like growth factor I in MCF-7 human breast cancer cells requires phosphatidylinositol 3-kinase and is independent of mitogen-activated protein kinase. J Biol Chem 272 (1997): 31163-31171.

Ellis S, Capuco AV. Cell proliferation in bovine mammary epithelium: identification of the primary proliferative cell population. Tissue Cell 34 (2002):155-163.

Etchebarne, BE. 2005 IGF-1 and leptin hormonal infusions alter the cell proliferation and transcriptional profile of the prepubertal bovine mammary gland. Ph.D Thesis. Michigan State University, East Lansing.

Fredlund, J., Johansson, M.C., Dahlberg, E. and Oredsson, S.M. Ornithine decarboxylase and S-adenosylmethionine decarboxylase expression during the cell cycle of Chinese hamster ovary cells. Exp Cell Res 216 (1995): 86–92.

Furlanetto RW. Receptor-mediated endocytosis and lysosomal processing of insulin-like growth factor I by mitogenically responsive cells. Endocrinology 122 (1988): 2044-2053.

Glimm DR, Baracos VE, Kennelly JJ. Northern and in situ hybridization analyses of the effects of somatotropin on bovine mammary gene expression. J Dairy Sci 75 (1992):2687-2705.

Grandis JR, Drenning SD, Chakraborty A, Zhou MY, Zeng Q, Pitt AS, Tweardy DJ. Requirement of Stat3 but not Stat1 activation for epidermal growth factor receptor-mediated cell growth in vitro. J Clin Invest 102 (1998): 1385-1392.

Grill CJ, Cohick WS. Insulin-like growth factor binding protein-3 mediates IGF-I action in a bovine mammary epithelial cell line independent of an IGF interaction. J Cell Physiol 183 (2000): 273-283.

Guler HP, Zapf J, Schmid C, Froesch ER. Insulin-like growth factors I and II in healthy man. Estimations of half-lives and production rates. Acta Endocrinol 121 (1989): 753-758.

Harper JV and Brooks G. The mammalian cell cycle: an overview. Methods Mol Biol 296 (2005): 113-153.

Harrison RD, Reynolds IP, Little W. A quantitative analysis of mammary glands of dairy heifers reared at different rates of live weight gain. J Dairy Res 50 (1983): 405-412.

Hauser SD, McGrath MF, Collier RJ, Krivi GG. Cloning and in vivo expression of bovine growth hormone receptor mRNA. Mol Cell Endocrinol 72 (1990): 187-200.

Hovey RC, Davey HW, Mackenzie DD, McFadden TB. Ontogeny and epithelial-stromal interactions regulate IGF expression in the ovine mammary gland. Mol Cell Endocrinol 136 (1998a): 139-144.

Hovey RC, DDS Mackenzie and TB McFadden. The proliferation of maouse mammary epithelial cells in response to specific mitogens is modulated by the mammary fat pad. In Vitro Cell Dev Biol Anim 34 (1998b): 385-392

Huber, M and Poulin R. Post-translational cooperativity of ornithine decarboxylase induction by estrogens and peptide growth factors in human breast cancer cells. Mol Cell Endocrinol 117 (1996): 211-218.

Huynh HT, Robitaille G, Turner JD. Establishment of bovine mammary epithelial cells (MAC-T): an in vitro model for bovine lactation. Exp Cell Res 197 (1991): 191-199.

Imagawa W, Spencer EM, Larson L, Nandi S. Somatomedin-C substitutes for insulin for the growth of mammary epithelial cells from normal virgin mice in serum-free collagen gel cell culture. Endocrinology 199 (1986): 2695-2699.

Jerome V, Leger J, Devin J, Baulieu EE, Catelli MG. Growth factors acting via tyrosine kinase receptors induce HSP90 alpha gene expression. Growth Factors 4 (1991): 317-327.

Kiess W, Haskell JF, Lee L, Greenstein LA, Miller BE, Aarons AL, Rechler MM, Nissley SP. An antibody that blocks insulin-like growth factor (IGF) binding to the type II IGF receptor is neither an agonist nor an inhibitor of IGF-stimulated biologic responses in L6 myoblasts. J Biol Chem 262 (1987): 12745-12751.

Klapper DG, Svoboda ME, Van Wyk JJ. Sequence analysis of somatomedin-C: confirmation of identity with insulin-like growth factor I. Endocrinology 112 (1983): 2215-2217.

Kurtz A, Vogel F, Funa K, Heldin CH, Grosse R. Developmental regulation of mammary-derived growth inhibitor expression in bovine mammary tissue. J Cell Biol 110 (1990): 1779-1789.

Kurtz A, Spitzer E, Zschiesche W, Wellstein A, Grosse R. Local control of mammary gland differentiation: mammary-derived growth inhibitor and pleiotrophin. Biochem Soc Symp 63 (1998): 51-69.

Kwok CF, Juan CC, Shih KC, Hwu CM, Jap TS, Ho LT. Insulin-like growth factor-1 increases endothelin receptor A levels and action in cultured rat aortic smooth muscle cells. J Cell Biochem 94 (2005): 1126-1134.

Lai A, Sarcevic B, Prall OW, Sutherland RL. Insulin/insulin-like growth factor-I and estrogen cooperate to stimulate cyclin E-Cdk2 activation and cell Cycle progression in

MCF-7 breast cancer cells through differential regulation of cyclin E and p21(WAF1/Cip1). J Biol Chem 276 (2001): 25823-25833.

Le Roith D, Bondy C, Yakar S, Liu J-L, Butler A. The Somatomedin Hypothesis: 2001. Endocr Rev 22 (2001): 53 - 74.

Lin FT, Daaka Y, Lefkowitz RJ. Beta-arrestins regulate mitogenic signaling and clathrin-mediated endocytosis of the insulin-like growth factor I receptor. J Biol Chem 273 (1998): 31640-31643.

Little W, Kay RM. The effects of rapid rearing and early calving on the subsequent performance of dairy heifers. Anim Prod 29 (1979): 131-142.

Maor G, Rochwerger M, Segev Y, Phillip M. Leptin acts as a growth factor on the chondrocytes of skeletal growth centers. J Bone Miner Res 17 (2002): 1034-1043.

Matitashvili E, Bramley AJ, Zavizion B. An in vitro approach to ruminant mammary gland biology. Biotechnol Adv 15 (1997): 17-41.

McGrath MF, Collier RJ, Clemmons DR, Busby WH, Sweeny CA, Krivi GG. The direct effect of insulin-like growth factors (IGFs) on normal bovine mammary epithelial cell proliferation and production of IGF binding proteins. Endocrinology 129(1991): 671-678.

Meares GP, Zmijewska AA, Jope RS. Heat shock protein-90 dampens and directs signaling stimulated by insulin-like growth factor-1 and insulin. FEBS Lett 574 (2004): 181-186.

Medema RH, Kops GJ, Bos JL, Burgering BM. AFX-like Forkhead transcription factors mediate cell-cycle regulation by Ras and PKB through p27kip1. Nature 404 (2000): 782-787.

Merlo GR, Graus-Porta D, Cella N, Marte BM, Taverna D, Hynes NE. Growth, differentiation and survival of HC11 mammary epithelial cells: diverse effects of receptor tyrosine kinase-activating peptide growth factors. Eur J Cell Biol 70 (1996): 97-105.

Messai H, Khatib AM, Lebrun G, Aubin P, Florina M, Jean F, Mitrovic DR. Endothelin-1 in monolayer cultures of articular chondrocytes from young and old rats: regulation by growth factors and cytokines. Mech Ageing Dev 114 (2000): 37-48.

Meyer MJ, Capuco AV, Ross DA, Lintault LM, Van Amburgh ME. Developmental and nutritional regulation of the prepubertal heifer mammary gland: I. Parenchyma and fat pad mass and composition. J Dairy Sci 89 (2006): 4289-97.

Muise-Helmericks RC, Grimes HL, Bellacosa A, Malstrom SE, Tsichlis PN, Rosen N. Cyclin D expression is controlled post-transcriptionally via a phosphatidylinositol 3-kinase/Akt-dependent pathway. J Biol Chem 273 (1998): 29864-29872.

Oredsson SM. Polyamine dependence of normal cell-cycle progression. Biochem Soc Trans 31 (2003): 366-370.

Pawitan Y, Michiels S, Koscielny S, Gusnanto A, Ploner A. False discovery rate, sensitivity and sample size for microarray studies. Bioinformatics 21 (2005): 3017-3024.

Petitclerc D, Chapin LT, Tucker HA. Carcass composition and mammary development responses to photoperiod and plane of nutrition in Holstein heifers. J Anim Sci 58 (1984): 913-9.

Plath-Gabler A, Gabler C, Sinowatz F, Berisha B, Schams D. The expression of the IGF family and GH receptor in the bovine mammary gland. J Endocrinol 168 (2001): 39-48.

Purup S, Sejrsen K, Akers RM. Effect of bovine GH and ovariectomy on mammary tissue sensitivity to IGF-I in prepubertal heifers. J Endocrinol 144 (1995):153-158.

Radcliff RP, VandeHaar MJ, Kobayashi Y, Sharma BK, Tucker HA, Lucy MC.Effect of dietary energy and somatotropin on components of the somatotropic axis in Holstein heifers. J Dairy Sci 87 (2004): 1229-35.

Reddy RK, Mao C, Baumeister P, Austin RC, Kaufman RJ, Lee AS. Endoplasmic reticulum chaperone protein GRP78 protects cells from apoptosis induced by topoisomerase inhibitors: role of ATP binding site in suppression of caspase-7 activation. J Biol Chem 278 (2003): 20915-20924.

Robinson RM, Akers RM, Forsten KE. Real-time detection of insulin-like growth factor-1 stimulation of the MAC-T bovine mammary epithelial cell line. Endocrine 13 (2000): 345-352.

Romagnolo D, Akers RM, Byatt JC, Wong EA, Turner JD. IGF-I-Induced IGFBP-3 potentiates the mitogenic actions of IGF-I in mammary epithelial MD-IGF-I cells. Mol Cell Endocrinol 102 (1994): 131-139.

Saiki RK, Walsh PS, Levenson CH, Erlich HA. Genetic analysis of amplified DNA with immobilized sequence-specific oligonucleotide probes. Proc Natl Acad Sci USA 86 (1989): 6230-6234.

Sejrsen K, Huber JT, Tucker HA, Akers RM Influence of nutrition of mammary development in pre- and postpubertal heifers. J Dairy Sci 65 (1982): 793-800.

Sejrsen K, Huber JT, Tucker HA. Influence of amount fed on hormone concentrations and their relationship to mammary growth in heifers. J Dairy Sci 66 (1983): 845-55.

Sejrsen K, Purup S. Influence of prepubertal feeding level on milk yield potential of dairy heifers: a review. J Anim Sci 75 (1997): 828-35.

Sejrsen K, Purup S, Vestergaard M, Foldager J. High body weight gain and reduced bovine mammary growth: physiological basis and implications for milk yield potential. Domest Anim Endocrinol 19 (2000): 93-104.

Shamay A, Cohen N, Niwa M, Gertler A. Effect of insulin-like growth factor I on deoxyribonucleic acid synthesis and galactopoiesis in bovine undifferentiated and lactating mammary tissue in vitro. Endocrinology 123 (1988): 804-809.

Silva LF. 2000 Role of leptin in mammary gland development in prepubertal heifers. Ph.D. Thesis. Michigan State University, East Lansing.

Silva LF, Liesman JS, Etchebarne BE, Nielsen MS, Vandehaar MJ. Short communication: intramammary infusion of IGF-I increases bromodeoxyuridine labeling in mammary epithelial cells of prepubertal heifers. J Dairy Sci 88 (2005): 2771-2773.

Sinha YN, Tucker HA. Mammary development and pituitary prolactin level of heifers from birth through puberty and during the estrous cycle. J Dairy Sci 52 (1969): 507-12.

Specht B, Bartetzko N, Hohoff C, Kuhl H, Franke R, Borchers T, Spener F. Mammary derived growth inhibitor is not a distinct protein but a mix of heart-type and adipocyte-type fatty acid-binding protein. J Biol Chem 271(1996): 19943-19949.

Smith JM, Van Amburgh ME, Diaz MC, Lucy MC, Bauman DE. Effect of nutrient intake on the development of the somatotropic axis and its responsiveness to GH in Holstein bull calves. J Anim Sci 80 (2002): 1528-37.

Stelwagen K, Grieve DG. Effect of plane of nutrition on growth and mammary gland development in Holstein heifers. J Dairy Sci 73 (1990): 2333-41.

Strange KS, Wilkinson D, Emerman JT. Mitogenic properties of insulin-like growth factors I and II, insulin-like growth factor binding protein-3 and epidermal growth factor on human breast epithelial cells in primary culture. Breast Cancer Res Treat 75 (2002): 203-212.

Stull MA, Richert MM, Loladze AV, Wood TL. Requirement for IGF-I in epidermal growth factor-mediated cell cycle progression of mammary epithelial cells. Endocrinology 143 (2002): 1872-1879.

Tivesten A, Bollano E, Andersson I, Fitzgerald S, Caidahl K, Sjogren K, Skott O, Liu JL, Mobini R, Isaksson OG, Jansson JO, Ohlsson C, Bergstrom G, Isgaard J. Liver-derived insulin-like growth factor-I is involved in the regulation of blood pressure in mice. Endocrinology 143 (2002): 4235-4242.

Tonner E, Barber MC, Allan GJ, Beattie J, Webster J, Whitelaw CB, Flint DJ. Insulin-like growth factor binding protein-5 (IGFBP-5) induces premature cell death in the mammary glands of transgenic mice. Development 129 (2002): 4547-57.

Umayahara Y, Kawamori R, Watada H, Imano E, Iwama N, Morishima T, Yamasaki Y, Kajimoto Y, Kamada T. Estrogen regulation of the insulin-like growth factor I gene transcription involves an AP-1 enhancer. J Biol Chem 269 (1994): 16433-16442.

Van Amburgh ME, Galton DM, Bauman DE, Everett RW, Fox DG, Chase LE, Erb HN. Effects of three prepubertal body growth rates on performance of Holstein heifers during first lactation. J Dairy Sci 81 (1998): 527-538.

Vandehaar MJ, Sharma BK, Fogwell RL. Effect of dietary energy restriction on the expression of insulin-like growth factor-I in liver and corpus luteum of heifers. J Dairy Sci 78 (1995): 832-41.

von Harsdorf R, Hauck L, Mehrhof F, Wegenka U, Cardoso MC, Dietz R. E2F-1 overexpression in cardiomyocytes induces downregulation of p21CIP1 and p27KIP1 and release of active cyclin-dependent kinases in the presence of insulin-like growth factor I. Circ Res 85 (1999): 128-136.

Weber MS, Purup S, Vestergaard M, Akers RM, Sejrsen K. Regulation of local synthesis of insulin-like growth factor-1 and binding proteins in mammary tissue. J Dairy Sci 83 (2000): 30-37.

Weber MS, Purup S, Vestergaard M, Ellis SE, Scndergard-Andersen J, Akers RM, Sejrsen K. Contribution of insulin-like growth factor (IGF)-I and IGF-binding protein-3 to mitogenic activity in bovine mammary extracts and serum. J Endocrinol 161 (1999): 365-373.

Weber MS, Purup S, Vestergaard M, Akers RM, Sejrsen K. Nutritional and somatotropin regulation of the mitogenic response of mammary cells to mammary tissue extracts. Domest Anim Endocrinol 18 (2000):159-64.

Williams JM and Daniel CW. Mammary ductal elongation: differentiation of myoepithelium and basal lamina during branching morphogenesis. Dev Biol 97 (1983): 274–290.

Wood TL, Richert MM, Stull MA, Allar MA. The insulin-like growth factors (IGFs) and IGF binding proteins in postnatal development of murine mammary glands. J Mammary Gland Biol Neoplasia 5 (2000): 31-42.

Woodward TL, Akers RM, Turner JD. Lack of mitogenic response to EGF, pituitary, and ovarian hormones in bovine mammary epithelial cells. Endocrine 2 (1994): 529-535.

Woodward TL, Xie J, Fendrick JL, Haslam SZ. Proliferation of mouse mammary epithelial cells in vitro: interactions among epidermal growth factor, insulin-like growth factor I, ovarian hormones, and extracellular matrix proteins. Endocrinology 141 (2000): 3578-3586.

Yee D, Paik S, Lebovic GS, Marcus RR, Favoni RE, Cullen KJ, Lippman ME, Rosen N. Analysis of insulin-like growth factor I gene expression in malignancy: evidence for a paracrine role in human breast cancer. Mol Endocrinol 3 (1989): 509-517.

Zadeh SM, Binoux M. The 16-kDa proteolytic fragment of insulin-like growth factor (IGF) binding protein-3 inhibits the mitogenic action of fibroblast growth factor on mouse fibroblasts with a targeted disruption of the type 1 IGF receptor gene. Endocrinology 138 (1997): 3069-3072.

Zapf J, Hauri C, Waldvogel M, Froesch ER. Acute metabolic effects and half-lives of intravenously administered insulinlike growth factors I and II in normal and hypophysectomized rats. J Clin Invest 77 (1986): 1768-1775.

Zavizion B, Politis I, Gorewit RC, Turner JD, Spitzer E, Grosse R. Effect of mammary-derived growth inhibitor on proliferation of MAC-T bovine mammary epithelial cells. J Dairy Sci 76 (1993):3721-3726.

Zavizion B, Gorewit RC, Politis I. Subcloning the MAC-T bovine mammary epithelial cell line: morphology, growth properties, and cytogenetic analysis of clonal cells. J Dairy Sci 78 (1995): 515-527.

Zhao X, McBride BW, Politis I, Huynh HT, Akers RM, Burton JH, Turner JD. Receptor binding and growth-promoting activity of insulin-like growth factor-I in a bovine mammary epithelial cell line (MAC-T3). J Endocrinol 134 (1992): 307-312.

Zong CS, Chan J, Levy DE, Horvath C, Sadowski HB, Wang L. Mechanism of STAT3 activation by insulin-like growth factor 1 receptor. J Biol Chem 275 (2000): 15099-15105.